DISTINCTIVE EXTINCTION PATTERNS OF LATE CRETACEOUS HYBODONTIFORM AND LAMNIFORM SHARKS IN NORTHERN GULF OF MEXICO CONTROLLED BY CHANGING MARINE PALEOENVIRONMENTS

by

CHELSEA MARIE COMANS

YUEHAN LU, COMMITTEE CHAIR
TAKEHITO IKEJIRI
W. JOE LAMBERT
SANDI SMART
THOMAS S TOBIN

A THESIS

Submitted in partial fulfillment of the requirements for the degree of
Master of Science in the Department of Geological
Sciences in the Graduate School of the
University of Alabama

TUSCALOOSA, ALABAMA

2021

ABSTRACT

Abundant fossil occurrences of Late Cretaceous sharks (Chondrichthyes, Elasmobranchii), especially Hybodontiformes and Lamniformes, in the northern Gulf of Mexico offer an ideal opportunity to study shark diversity patterns leading up to the end-Cretaceous mass extinction. Here, we present a dataset representing 16 genera and 25 species (five hybodontiforms and 20 lamniforms). Species counts and extinction and origination rates are quantified across the Coniacian to Danian. Both groups display an overall increasing trend of extinctions that peak in the Campanian (e.g., the 'Middle Campanian Crisis': MCC) but show noticeable differences concerning the magnitude and relative timings. Hybodontiforms show increased diversity losses from the Santonian to middle Campanian before regionally disappearing during the entire Maastrichtian. Lamniforms declined in diversity in the early to middle Campanian (about half the magnitude of the hybodontiform losses) and the end-Maastrichtian. For both taxa, originations declined from the Santonian to middle Campanian and remained near zero toward the end-Cretaceous. Statistical analyses (correlation tests, principal component analysis) were used to determine the potential importance of marine environmental changes, such as sea level, sea surface temperature, marine productivity on the two different extinction trends of hybodontiforms and lamniforms. Lamniform diversity loss is negatively correlated with globally decreasing sea levels. Hybodontiform diversity loss is positively correlated with globally increasing sea levels. Sustained fluctuations in marine productivity and

sea surface temperature in the Gulf of Mexico may have contributed to low origination rates for lamniforms following the MCC. Previously published occurrences in upper Campanian to upper Maastrichtian strata in the Northern Atlantic coast indicate that few species did not become extinct globally. This study suggests that changing marine paleoenvironments (esp., sea level changes) could have had a big impact on Cretaceous sharks (particularly benthic durophagous forms that lived in near-shore environments) due to newly emerged unsuitable habitats.

DEDICATION

This thesis is dedicated to my family and friends who have been a constant encouragement throughout the creation of this manuscript. This manuscript is also dedicated to Nicholas Hood and all those whose dreams were cut tragically short.

LIST OF ABBREVIATIONS AND SYMBOLS

K-Pg	Cretaceous-Paleogene
MS	Multiton Subsampling
m	Meters
Ma	Millions of years
Myr	million years
OMZ	Oxygen minimum zone
p	Per-Capita origination rate per million years
$P_{Em.y.}$	Proportional extinction rate per million years
$P_{Om.y.}$	Proportional origination rate per million years
q	Per-Capita extinction rate per million years
SQS	Shareholder Quorum Subsampling
WIS	Western Interior Seaway
$\delta^{13}C$	Ratio of ^{13}C to ^{12}C isotopes relative to PDB reported in per mil
$\delta^{18}O$	Ratio of ^{18}O to ^{16}O isotopes relative to SMOW reported in per mil
‰	Per mil (Parts per thousand)
µ	Quorum

ACKNOWLEDGEMENTS

I would like to give a special thank you to everyone who helped me to complete this thesis research and manuscript. Firstly, thank you to my thesis advisor, Dr. YueHan Lu, and Dr. Takehito Ikejiri for allowing me the opportunity to work with them. Dr. Ikejiri has provided me with so many opportunities to work in the field and provided community outreach opportunities with the Alabama Museum of Natural History Summer Expedition program. Dr. Lu has provided me with the resources and knowledge to bring my paleo-centered, geochemical ideas into reality.

I also would like to thank my research group and other department friends and colleagues for their help and encouragement. Dr. Man Lu, Dr. Shuo Chen, Jian Chen, and Sakinat Ahmad have all been so helpful. They've encouraged me throughout this process and just taken the time to show me where lab equipment was.

I am not sure there are words enough to thank my family for all that they have done. Without their encouragement and support, I probably would not have gone to graduate school, let alone completed my degree.

Lastly, none of this would have been possible without the help of my most generous funding sources. I would like to thank the University of Alabama National Alumni Association, the University of Alabama Graduate School, the Department of Geological Sciences at the University of Alabama, and the Gulf Coast Association of Geological Societies.

TABLE OF CONTENTS

LIST OF TABLES

LIST OF FIGURES

1. INTRODUCTION

Sharks are a diverse group of Chondrichthyes (cartilaginous fishes) that first appeared in the very Late Devonian (Maisey, 2012). Hybodontiforms represent some of the earliest shark taxa and are considered a sister group of modern sharks (neoselachians) (Maisey, 2012). They dominated marine populations until neoselachians appeared in the Triassic (Rees and Underwood, 2008; Guinot, 2013). Some research has suggested that neoselachians first appeared as early as the Permian (e.g., Guinot et al., 2012; Guinot, 2013), but this idea is based on limited fossil occurrences (see Ivanov, 2005). During the Jurassic to Cretaceous, neoselachians dominated the marine selachian (all sharks) populations (Rees and Underwood, 2008; Maisey, 2012). The Early Cretaceous was a particularly critical time for neoselachian evolution, especially for lamniforms that went through multiple radiation events through the Late Cretaceous (Rees, 2006; Underwood, 2006; Guinot, 2013). Lamniforms, or Mackerel sharks, are assigned to a crown group that includes such modern species as *Carcharodon carcharias* (the great white shark) and *Carcharias taurus* (the sand tiger shark). The radiation of lamniforms and other modern shark taxa that began during the Late Jurassic coincided with a decline of hybodontiform sharks towards the end-Cretaceous (Rees and Underwood, 2008; Masiey, 2012). All hybodontiforms had gone extinct by the end-Cretaceous, regarded as victims of the K-Pg mass extinction (Rees and Underwood, 2008). To date, the exact processes (i.e., the timing and mechanisms) of a possible faunal turnover between hybodontiforms and lamniforms in the Late Cretaceous remains unclear.

A recent paper examining marine vertebrate diversity in the northern Gulf of Mexico found a significant decline in lamniforms, hybodontiforms, many bony fishes, and some marine reptiles during the Middle Campanian (i.e., 'the Middle Campanian Crisis' coined by Ikejiri et al., 2020). Based on Late Cretaceous marine vertebrate diversity data presented by the authors, the decline of Late Cretaceous hybodontiform taxa may not be driven only by the radiation of lamniform taxa. Such studies indicate a much broader cause of diversity loss, at least at the onset stage, such as paleoenvironmental changes that disproportionately affected specific shark taxa. However, the spatiotemporal patterns of hybodontiform and lamniform evolution have not been studied in detail for this possible faunal turnover in the Late Cretaceous. Here, we investigate if the MCC was a key late-stage event for the transition from hybodontiform to lamniform dominance in the northern Gulf of Mexico and compare our diversity data with possible global paleoenvironmental changes that could control diversity trends.

Fossil assemblages from various Upper Cretaceous sites producing both hybodontiform and lamniform fossils suggest that they occupied the same paleogeographic regions with possibly overlapping habitats (see Thurmond and Jones, 1981; Case and Schwimmer, 1988; Ciampagalio et al., 2013; Ikejiri et al., 2013; Cicimurri et al., 2014). Cretaceous hybodontiforms likely inhabited shallow, nearshore environments, where they dwelled at the bottom of the water column (Fischer, 2008). Lamniforms were pelagic and occupied a broader range of habitats, from shallow, coastal waters to deeper waters (e.g., Maisey, 2012; Klimley, 2013). The dominance of the deeper-water environments by radiating lamniforms has been suggested to have forced hybodontiforms into shallower waters while competing for available resources during the Late Cretaceous (e.g., Rees and Underwood, 2008; Maisey, 2012; Guinot, 2013). Marginalizing hybodontiforms to nearshore environments, where resources may have been

scarce, could have increased competition with lamniforms and ultimately lead to hybodontiform extinction. Other studies have suggested rapidly changing marine paleoenvironments (e.g., sea-level changes, sea surface temperature fluctuations, marine productivity shifts) contributed to the diversity losses among marine vertebrates (e.g., Jablonski and Raup, 1995; Alegret et al., 2011; Haq, 2014). However, it remains unclear how the faunal turnover from hybodontiforms to lamniforms occurred (e.g., the diversity pathways) or what possible driving factors controlled the transition.

Regarding possible abiotic controlling factors for Late Cretaceous shark diversity, the important question remains if they affect only regional or global areas. Several global-scale studies have investigated the causes of neoselachian diversification throughout the Cretaceous and Cenozoic, but they focus on later shark evolution (e.g., Kriwet and Benton, 2004; Belben et al., 2017; Bazzi et al., 2018; Condamine et al., 2019). Regional studies that focus on the process of faunal turnover from selachians (hybodontiforms) to neoselachians (especially lamniforms) in the Late Cretaceous are limited but do identify diversity declines starting in the early Campanian (e.g., Guinot, 2013; Ikejiri et al., 2020). Guinot (2013) attributed high species diversity in the Santonian units of the Anglo-Paris Basin, northwestern Europe, and the Western Interior Seaway (WIS) to warming sea temperatures and low diversity in the early Campanian to rapid sea temperature decreases. Moreover, Ikejiri et al. (2020) suggested that changing sea levels across the latest Cretaceous resulted in fluctuations in species diversity, particularly in bony and cartilaginous fishes. Regional-scale studies like those of Guinot (2013) and Ikejiri et al. (2020) can reveal higher temporal and spatial resolution information and yield insights unrevealed from global-scale studies. However, neither study investigated any paleoenvironmental driver in detail for their diversity patterns.

Here, we investigate the diversity patterns of hybodontiform and lamniform sharks in the northeastern Gulf of Mexico across the last 20 million years of the Late Cretaceous using a dataset of over 2,500 specimens representing 25 species and 16 genera from Alabama in the southeastern U.S.A. Alabama has a robust Late Cretaceous fossil record because of its environmental and depositional setting, which was favorable for the preservation of marine vertebrate fauna (e.g., Applegate, 1970; Shimada and Hooks, 2004; Shimada, 2009; Ebersole and Dean, 2013; Ikejiri et al., 2013; Ciampagalio et al., 2013; Ikejiri et al., 2020). We first answer the question of when the greatest diversity losses (i.e., highest extinction values) occurred in each group of Late Cretaceous sharks. We quantify the exact victims of shark taxa and the magnitude of the MCC, which may be a key time interval for the faunal turnover from hybodontiforms to lamniforms. Understanding the temporal patterns of lamniform and hybodontiform diversity in a selected paleogeographic area leads to the investigation of possible driving factors that relate to Late Cretaceous marine paleoenvironmental changes, such as changes in sea levels, sea surface temperatures, and primary marine productivity. Our regional study offers a unique bottom-up approach that provides new insight into missing information left by top-down, global-scale studies.

2. GEOLOGIC SETTING

The study area is the current geographic position of Alabama, which was part of the northern Gulf Coast of Mexico basin during the Late Cretaceous. Upper Cretaceous units crop out along the central region of the state from the northwest to central-eastern portions and form a crescent-shape distribution (Fig. 1). Units dip slightly south to southwest (Mancini et al., 1996) and decrease in age from north to south, recording a major sea-level regression across the Late Cretaceous to Paleogene. There are five fossil-bearing marine formations and three members, which represent near-continuous stratigraphic sequence from the Coniacian to Maastrichtian (Table S1). Earlier Late Cretaceous stages (i.e., Turonian and Cenomanian) do not have any surface rocks exposed in Alabama, and thus no Late Cretaceous shark fossil occurrences are found below the latest Coniacian strata.

The stratigraphy and lithology of western and central Alabama differ from that of eastern Alabama, indicating possibly different depositional environments (Raymond et al., 1988; Ikejiri et al., 2020). To investigate diversity dynamics, this study focuses only on occurrences from western and central Alabama (see Fig. 1). Western and central Late Cretaceous units were under near-constant environmental and depositional settings across the study period (i.e., deposition of chalk and marl abundant units representing inner to middle neritic paleoenvironmental settings; Table S1). Formations found only in eastern Alabama represent a shallower near-shore marine setting (Liu, 2009) than the inner to middle neritic environments of the central and western portions (Mancini et al., 1996). Units restricted to eastern Alabama (e.g., Blufftown Formation, Providence Sand Formation) crop out starting east of Montgomery County. We, therefore, define western and central Alabama as geologic units west of and including Montgomery County to the Alabama-Mississippi border (Fig. 1).

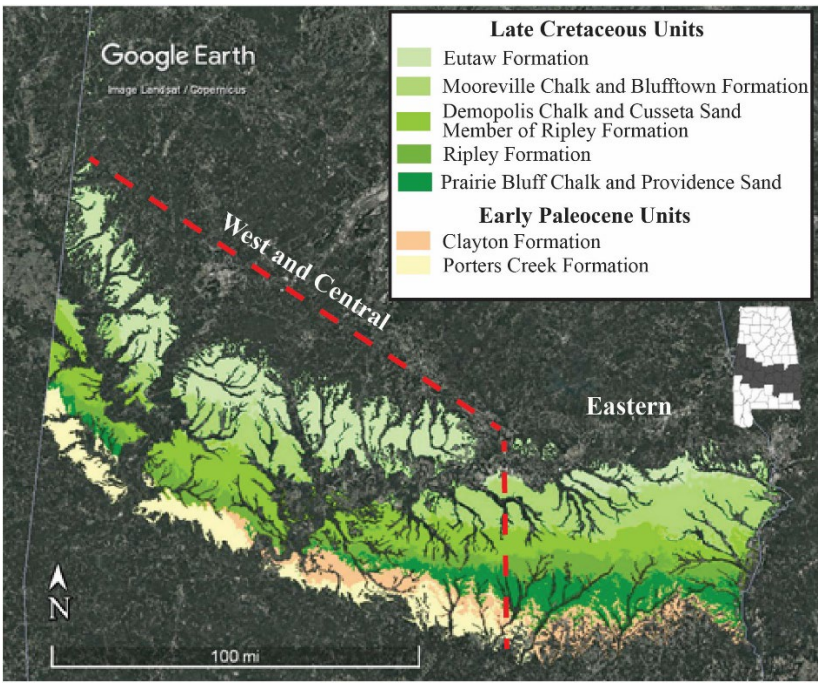

Fig. 1. Geologic map of Upper Cretaceous and lower Paleocene units in Alabama. Upper Cretaceous units that only outcrop in eastern Alabama are not shown. The dashed red line indicates the central and western portions of the state where fossil occurrences were analyzed for this study. Map data are from the USGS Geologic Maps of U.S. States (Horton, 2017).

In western and central Alabama, the Coniacian through late Maastrichtian record exhibits at least three transgressive-regressive cycles and potentially four unconformities (Mancini and Puckett, 2002): mid-Coniacian, middle Campanian, upper Campanian to lower Maastrichtian, and upper Maastrichtian strata (Fig. 2). The first depositional hiatus is a disconformity below the Eutaw Formation during the lower Coniacian, which explains the limited number of exposed outcrops from which fossils are present. A second unconformity exists in the lower Demopolis Chalk Formation of western Alabama but is not observed in central Alabama (Mancini et al., 1995, 1996). The middle to upper Campanian and lower to upper Maastrichtian unconformities

occur in the middle of the Ripley Formation across the Campanian-Maastrichtian boundary and the contact between the Maastrichtian Prairie Bluff Chalk and the Paleocene Clayton Formation.

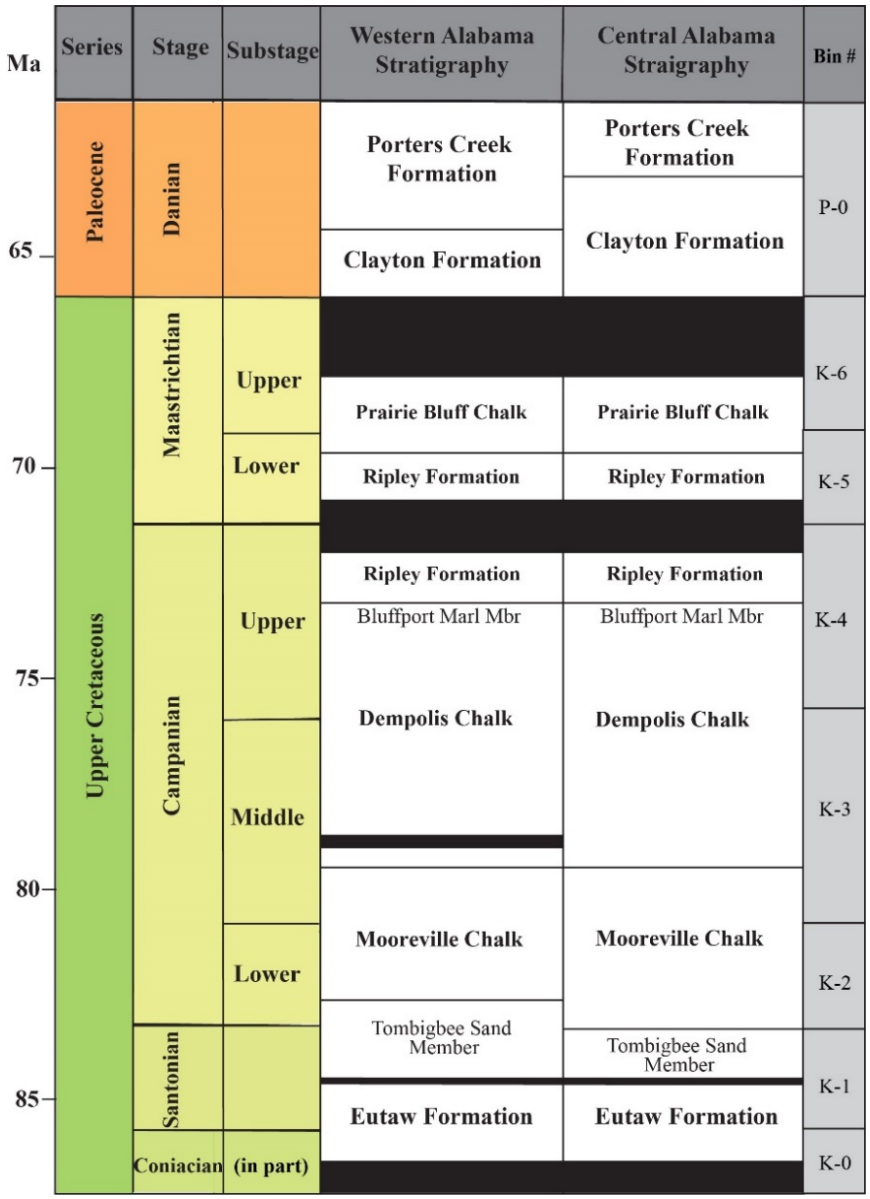

Fig. 2. Stratigraphy of Upper Cretaceous and lower-most Paleocene units in western and central Alabama. The eight time-bins established for this study (K-0 to P-0) are based on substage intervals. The ages and stratigraphy of geologic formations and members is based on Raymond et al. (1988), Mancini et al. (1996), and Mancini and Puckett (2005).

3. MATERIALS AND METHODS

3.1. Shark fossil occurrences

We modified data on Late Cretaceous hybodontiforms and lamniforms from the northern Gulf of Mexico published by Ikejiri et al. (2020). That dataset includes museum specimens collected in Alabama curated through 2015. We added specimens curated between 2015 and 2019 to the existing dataset and verified the taxonomic identification via visual inspection. New specimen occurrences were primarily from the Alabama Museum of Natural History and McWane Science Center (Table S2). Specimens with uncertain identification (i.e., broken or weathered specimens) at least at the generic level were excluded, and where possible, specific level identifications were made. Monospecific genera identifications were assigned to their single known species. Polyspecific genera identifications not identifiable to the specific level were excluded. There has been some debate over the higher classification of the genus Ptychodus and whether it should be considered a Hybodontiformes (e.g., Shimada, 2012), Neoselachiian (e.g., Hoffman et al., 2016), or a new group, Ptychodontiformes (e.g., Hamm and Harrell, 2013). Here, we adopt the traditional view that Ptychodus is a member of Hybodontiformes (Patterson, 1966; Cappetta, 1987) because no other definitive idea of the higher-level classification has been available (see further discussion in Maisey et al. (2004) and Shimada (2012)). We excluded specimens that did not have reliable or verifiable locality information on fossil sites and stratigraphic occurrences. The dataset included, in total, 3,328 specimens from 14 different museum collections (Table S2). Only 2,619 specimens met our minimum sampling criteria requirements.

Our stratigraphic resolution for diversity analyses was the Stage-level, and occurrence data were organized into eight stage-based time-bins using collection site information (Fig. 2). Of the eight-time bins, seven time-bins represent Late Cretaceous stages: Coniacian (K-0),

Santonian (K-1), early Campanian (K-2), middle Campanian (K-3), late Campanian (K-4), early Maastrichtian (K-5), late Maastrichtian (K-6). One time-bin represents the Paleocene Danian stage (P-0). The purpose of bins K-0 and P-0 is to assess the presence of singleton taxa (i.e., species that occurred only in a single time interval, which may reflect strong bias; Foote, 2000; Foote and Miller 2007) in bins K-1 and K-6 (e.g., Foote, 1999, 2000; Ikejiri et al., 2020). Fossil occurrences from the Coniacian of Alabama are largely absent due to a depositional hiatus (Raymond et al., 1988; Mancini et al., 1995, 1996; Mancini and Puckett, 2002). When specimens occurred in the Santonian but not Coniacian of Alabama, we included data from Coniacian strata in surrounding Gulf Coast states (e.g., Texas, Mississippi, Georgia) to verify whether a specimen was a singleton taxon or simply not present in the northern Gulf of Mexico. Using age-based time-bins is an effective method for organizing occurrence data to show changes in diversity and paleoecology by providing higher resolution analyses than formation-based intervals (e.g., Kiessling and Aberhan, 2007a, b; Kiessling et al., 2007; Clapham and Payne, 2011; Freymueller et al., 2019).

3.2. Subsampling and data validation

Assessing potential biases in our dataset is an essential part of data validation (Raup, 1991). We used a variety of subsampling and sampling variations to assess taxonomic richness and sample completeness. Taxonomic richness uses 'range-through,' 'sampled-in-bin,' and 'corrected sampled-in-bin' species counts. 'Sampled-in-bin' counts the number of taxa in a specific time-bin, but it does not consider Lazarus taxa (i.e., taxa that appear in nonconsecutive time-bins). 'Range-though' accounts for Lazarus taxa by assuming that a fossil taxon ranges through its first and last appearances (Foote and Miller, 2007). 'Corrected sampled-in-bin' is partially corrected using three-timer sampling-completeness (Alroy et al., 2001) for such biases

as incomplete sampling and the use of discretized time intervals. Classical rarefaction analysis of raw species data was completed using PAST (version 4.02: Hammer et al., 2001) to assess whether the data set is robust enough to investigate diversity patterns. The number of species typically increases as sample size increases. Rarefaction assesses whether the same number of species would be found in a smaller sample size.

We compared classical rarefaction results to Shareholder Quorum Subsampling (SQS) (Alroy, 2010a) and Multiton Subsampling (MS) (Alroy, 2017a). SQS was completed using an R code provided by Alroy (2010b) and MS using an R code provided by Alroy (2017b). SQS has become a widely applied subsampling method to determine relative richness suppression or completeness in the fossil record. These methods stem from frequency coverage and use coverage levels, or quorums, that range from zero to one. "Coverage" (Good 1953) is defined as the frequencies of the species sampled. A taxon is only credited in the coverage the first time it is drawn (Alroy, 2010a). Thus, sampling levels concern coverage, and once that level of sampling is achieved it represents a quorum. SQS does not yield realistic counts like those of raw species pool counts. Instead, it provides fair, although uneven, sampling by drawing on a random fraction of true pool size to produce relative diversity estimates. The quorum, q, was set as 0.2, 0.4, 0.6, and 0.8 with 1000 iterations for each dataset using two-timer species counts (Alroy, 2010a) with and without singletons.

Multiton subsampling is a more robust subsampling method. It is like its predecessor SQS in its ability to decompress the data but has shown to be more precise and less biased when assessing diversity of data sets with very high or low richness levels (Alroy, 2017a). MS uses target ratios that range from zero to one and are equivalent to quorum levels. Target ratios are the total number of species divided by the number of species with more than one specimen in the

sample. Global datasets require smaller (less than 0.4) target ratios (Alroy, 2017a; Freymueller et al., 2019). However, the data presented here is from a small regional dataset and thus requires a quorum level greater than 0.4. To objectively define a target for all time-bins, the target was calculated from the early Campanian data for all shark species and genera (hybodontiforms + lamniforms). The early Campanian has the highest number of occurrences and thus is least likely to be affected by under-sampling. Targets calculated for species and generic levels were 0.96 and 0.94, respectively. Given the small sample sizes of our data set, the target ratios calculated could violate the principle that sampling quality should increase with the raw data (Alroy, 2017a). It is then necessary to multiply the target ratios by $N_i/(S_{I,i}+1)$, where N_i is the sample size (or the number of individuals considered) and $S_{I,i}$ is the expected number of singletons to be found in N_i. Here, the species target ratio was multiplied by 6.25 and yielded a final target of 6. The generic target ratio was multiplied by 45.0 and yielded a final target ratio of 4.7.

3.3. Extinction and origination rates

Extinction and origination rates are quantified in each of the six primary time-bins (K-1 to K-6 in Fig. 2) for taxa assigned to hybodontiforms (including the genus *Ptychodus*) and lamniforms. Extinction and origination percentages are calculated in each time-bin by dividing the number of species that originate or become extinct in a particular time-bin by the total number of species occurring in that same bin (e.g., Foote, 2000; Ikejiri et al., 2020). Species occurrences with and without singletons were analyzed separately and compared. All species data are analyzed and compared to finer groupings (lamniforms and hybodontiforms, separately). Analyses were done using RStudio (R Core Development Team, 2020) and the R-package 'divDyn' (Kocsis et al., 2019). Multiple metrics are employed to assess and compare taxonomic turnover rates. Calculated extinction and origination rates for hybodontiforms and lamniforms

combined include proportional, per-capita (Foote, 1999; Foote, 2000), three-timer (Alroy, 2008), corrected three-timer (Alroy, 2008), gap-filler (Alroy, 2014), and second-for-third (Alroy, 2015). Proportional and per-capita rates are used for finer grouping analyses.

By examining hybodontiform and lamniform diversity patterns separately, principal information about the differences in their diversity patterns is revealed. For example, identifying the timing of diversity peaks (e.g., highest extinction interval) for each group or comparing the diversity patterns of taxa with each group (e.g., *Ptychodus* vs. *Meristodonoides* in hybodontiforms). Which species or genera survive and which become extinct is of particular interest to faunal turnover events. We then formulate a series of questions to investigate what, if any, paleoenvironmental drivers may contribute to overall or individual groups' extinction patterns. Lastly, we discuss taxa identified as singletons and the possible biases they present to diversity patterns.

3.4. Statistical analysis of paleoenvironmental factors

Paleoenvironmental factors such as changing sea surface temperatures, sea levels, and marine productivity often contribute to extinction and origination trends in marine animals (Benton, 2009; Benson and Butler, 2011; Kelley et al., 2014). Data on global sea level estimates (Haq, 2014) and $\delta^{18}O$ and $\delta^{13}C_{carb}$ (Prokoph et al., 2008) from the Santonian and Danian are statistically compared to lamniform and hybodontiform extinction and origination patterns (i.e., proportional and per-capita extinction and origination rates). Three correlation tests (Pearson's linear, Spearman's rho rank, and Kendall's tau rank) are used to compare the magnitudes of the three paleoenvironmental factors for their impact on shark diversity. The correlation coefficients of the three different correlation tests (Pearson's r, Spearman's ρ, and Kendall's τ) determines the level of correlation (e.g., weak, moderate, strong), and P-values determine if any correlations

were statistically significant ($P < 0.05$). We analyzed only statistically significant correlations with high or very high correlation coefficients as potential diversity controls. Principal component analysis (PCA) is a useful tool to visualize multivariate data (i.e., strength and direction of correlations) among variables grouped time-bins (e.g., Lu et al., 2021). PCA is ran using the same data matrix to compare relative relations of the extinction and origination trends hybodontiforms and lamniforms and three paleoenvironmental parameters through the K-1 to P-0 intervals. All analyses are run using the PAST (version 4.02: Hammer et al., 2001).

4. RESULTS

4.1. Relative abundance of Late Cretaceous sharks

Of the Cretaceous marine vertebrate fossil record, sharks are the most abundant group in Alabama (Ikejiri et al., 2013; 2020). In our dataset, 2,619 specimens are assigned to either lamniforms or hybodontiforms (n = 2,251 and 368, respectively). Rarefaction analyses include three different curves: both groups (27 total species), lamniforms (20 species), and hybodontiforms (seven species). All three curves showed a sufficiently large sample size relative to the total species counts (Fig. 3).

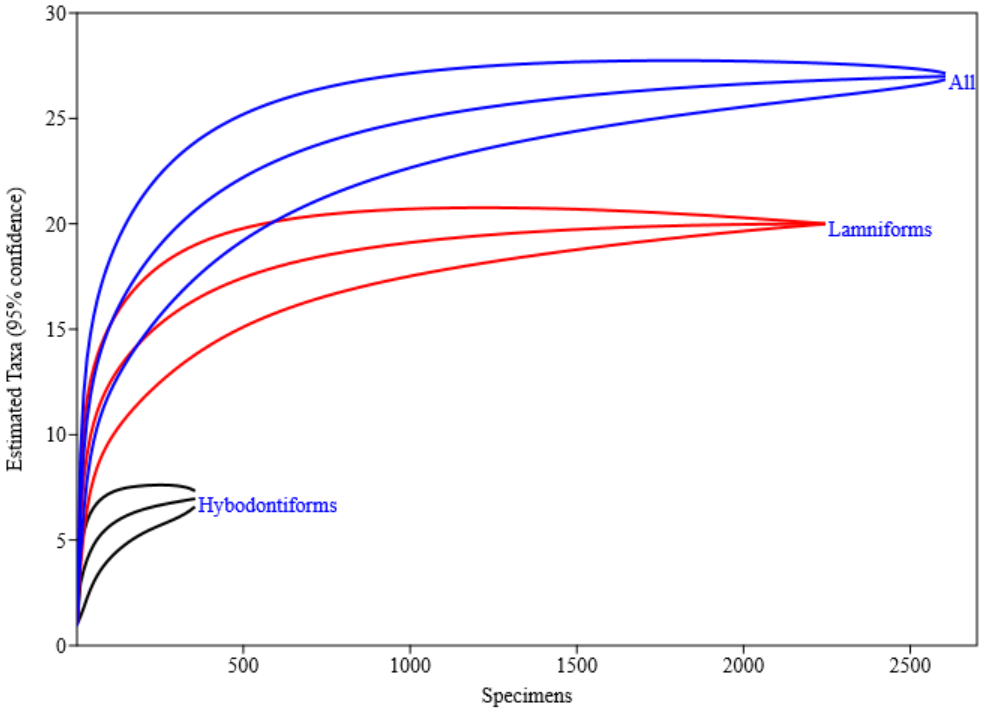

Shareholder quorum subsampling (SQS) assesses a topology of the overall species occurrence in each of the six time-bins (K-1 to K-6) (Fig. 4). SQS curves at four different quora with and without singletons for all shark species, lamniform, and hybodontiform species show similar overall patterns (e.g., the highest in the Santonian, the lowest in the Early Maastrichtian; a large drop between the early to middle Campanian) (Table S6). Those features were observed in the datasets of both with and without singletons, suggesting that those species with single-unit occurrences do not affect further quantification of taxonomic rates. The two shark subgroups (lamniforms and hybodontiforms) show different patterns, which indicates our dataset is a reasonably robust sample size. If the patterns for each sub-group were the same, it would indicate sampling or preservational biases. To sum, the proposed dataset of 2,619 shark specimens is substantial enough to assess diversity analyses (Fig. 4).

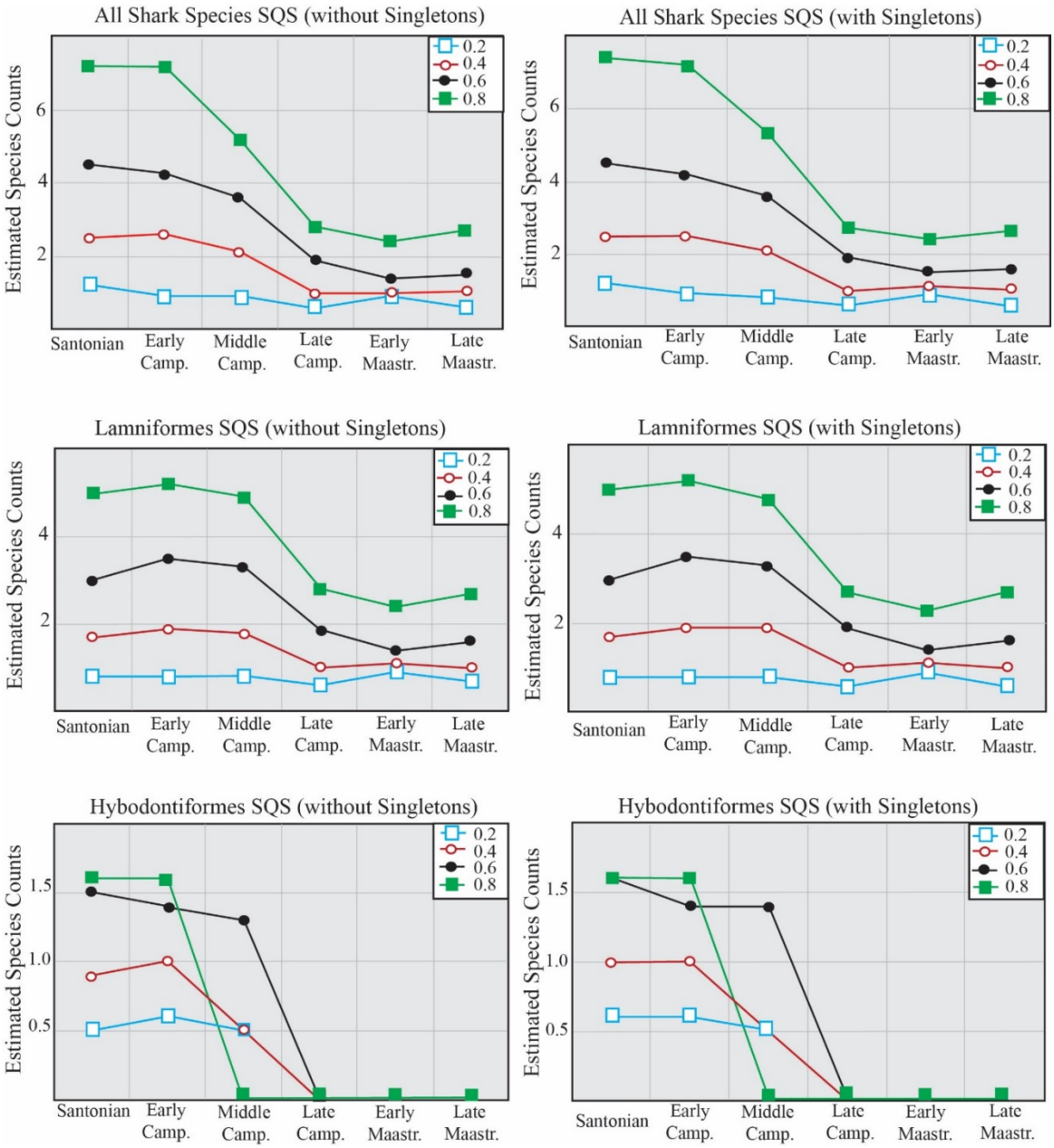

Lastly, multiton subsampling (MS) assesses the robusticity of a dataset using similar topology interpretations as SQS (Fig. 5). MS is considered a more robust subsampling method

for smaller or regionally based datasets (Alroy, 2017a). Overall, MS diversity patterns strongly resemble those seen in SQS (Fig. 4) and further confirm the robustness of the proposed dataset. To sum, the proposed dataset of 2,619 specimens is substantial enough to assess diversity analyses.

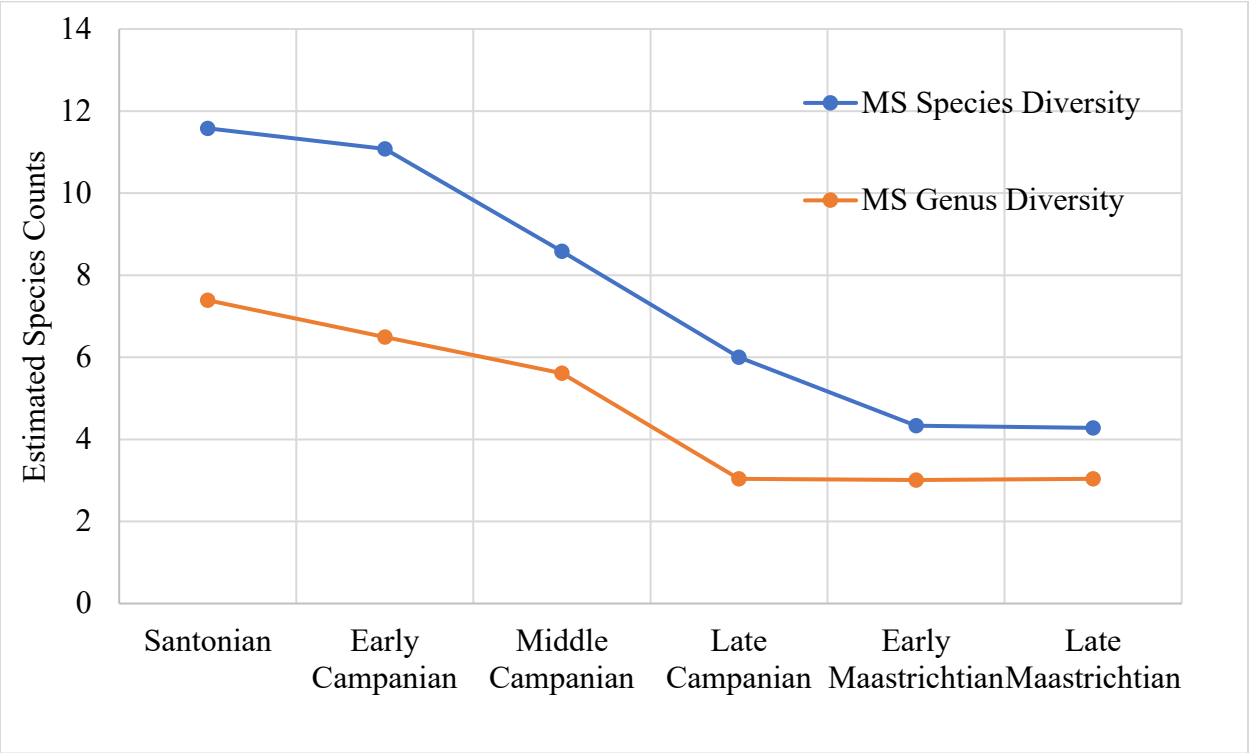

Fig. 5. Multiton Subsampling (MS) for species and genus level richness. Estimates include singleton taxa. The target for all time-bins was based on the Early Campanian. The specific and generic targets were set at 6 and 4.7, respectively. Raw MS data for species and genus levels are available in Table S8.

4.2. Shark fossil occurrences

The taxonomic richness of Late Cretaceous sharks is quantified by sampling taxa based on 'range-through,' 'sampled-in-bin,' and 'corrected sampled-in-bin' numbers (e.g., Foote, 1999 and Alroy, 2014) from taxonomic counts at the specific and generic levels of both hybodontiforms and lamniforms with singletons (Fig. 6; Table S9). All richness curves indicate

the highest species abundance is in the Santonian to early Campanian (n = 23 species). Species abundance then declines from the middle Campanian to late Maastrichtian. The highest generic richness is also in the Santonian to early Campanian intervals (approximately 15 genera). The greatest decrease in taxonomic richness occurred from the early to middle Campanian. The 'sampled-in-bin' counts increased following the middle Campanian decline and before the end-Cretaceous mass extinction. This trend is also seen in the 'corrected sampled-in-bin' data but not the 'range-through' data. Following the middle and late Campanian, species and generic richness remained low and continued to decline.

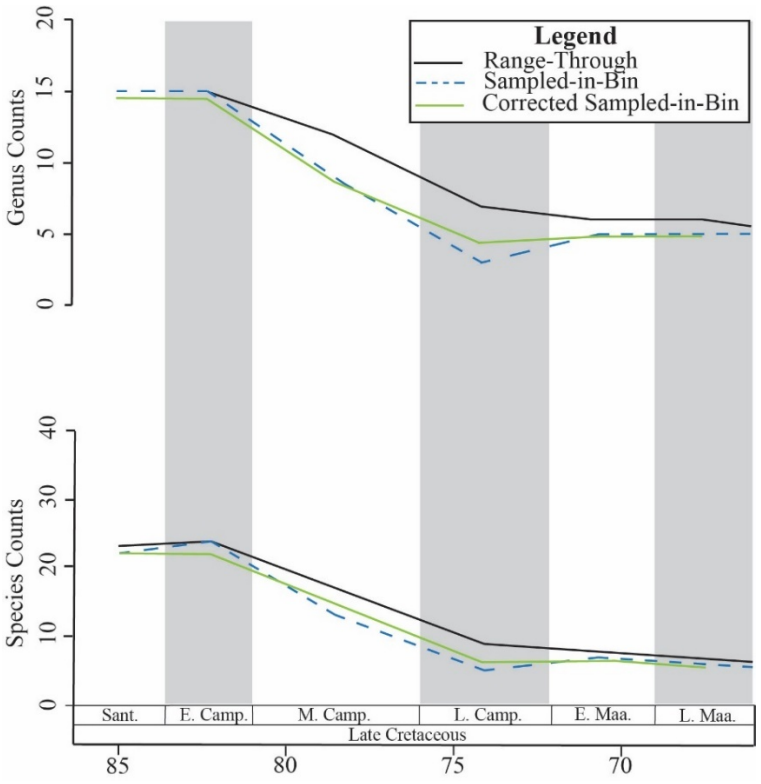

Fig. 6. Taxonomic counts of Late Cretaceous sharks in northern Gulf of Mexico. All species are represented by range-through, sampled-in-bin, and corrected sampled-in-bin. **Top**: Genus Richness. **Bottom**: Species richness. Coniacian and Paleocene are omitted.

Of the 3,328 total specimens examined, 2,619 are used to assess diversity dynamics. These occurrences were all identified to the generic and specific levels when available.

Lamniforms account for most of the recorded data, representing 2,251 occurrences. Hybodontiforms account for 368 occurrences (Table 1). The highest number of specimens for both taxa occurred in the K-2 (early Campanian) interval and, the lowest number occurred in the P-0 (Danian). The highest number of species and genera occurred in the K-1 (Santonian) and K-2 intervals, and the lowest occurred in P-0.

Bin #	Age	Duration (Myr)	Total Occ.	Lamniform Occ.	Hybodontiform Occ.	Genus & Species Counts
P-0	Danian	4.4	15	15	0	4 gen., 4 spp.
K-6	Late Maastrichtian	3.0	34	34	0	4 gen., 6 spp.
K-5	Early Maastrichtian	3.1	90	90	0	4 gen., 7 spp.
K-4	Late Campanian	3.9	28	28	0	4 gen., 8 spp.
K-3	Middle Campanian	5.0	124	120	4	9 gen., 16 spp.
K-2	Early Campanian	2.6	1605	1408	197	13 gen., 23 spp.
K-1	Santonian	2.7	555	419	136	15 gen., 23 spp.
K-0	Coniacian	3.5	168	137	31	10 gen., 11 spp.
	Total		**2619**	**2251**	**368**	

Table 1. Taxonomic counts and specimen occurrences (Occ.) of Late Cretaceous lamniforms, hybodontiforms, and both shark groups from northern Gulf of Mexico with respect to eight time-bins (K-0 to P-0).

In total, including singletons, 16 genera and 27 species were identified (Table S3). Of the 27 species identified, 20 species represent lamniforms, and seven species represent hybodontiforms. There are only two singleton taxa found in our dataset (both hybodontiforms): *Ptychodus whipplei* and *Ptychodus mammillaris*. The raw species counts with and without singletons showed that the highest number of species occurred in the Santonian (n = 23 and n = 22) and early Campanian (n = 23 and n = 22) (Table S5). With and without the two singletons,

the fewest of species occurrences were in the late Campanian (n = 8), early Maastrichtian (n = 7), and late Maastrichtian (n = 6).

Stratigraphic ranges estimated for each taxon showed some species' last occurrence was in the early to middle Campanian (Fig. 7). In the early Campanian, six species, not including singletons, had their last occurrence. Of the six species, three were hybodontiforms (*Ptychodus polygyrus*, *Ptychodus rugosus*, and *Lonchidion cristatum*), and three were lamniforms (*Squalicorax lindstromi*, *Scapanorhynchus rapax*, and *Protolamna borodini*). In the middle Campanian, eight species had their last occurrence, including six lamniforms (*Squalicorax falcatus*, *Scapanorhynchus raphiodon*, *Pseudocorax laevis*, *Pseudocorax affinis*, *Paranomotodon angustidens*, and *Archaeolamna kopingenesis*) and two hybodontiforms (*Ptychodus mortoni* and *Meristodonoides multiplicatus*). After the middle Campanian, there were no hybodontiform occurrences. Excluding singletons, no new species appeared from the middle Campanian to the end-Maastrichtian. Only two species survived through the end-Cretaceous mass extinction, namely *Cretalamna appendiculata* and *Carcharias* sp.

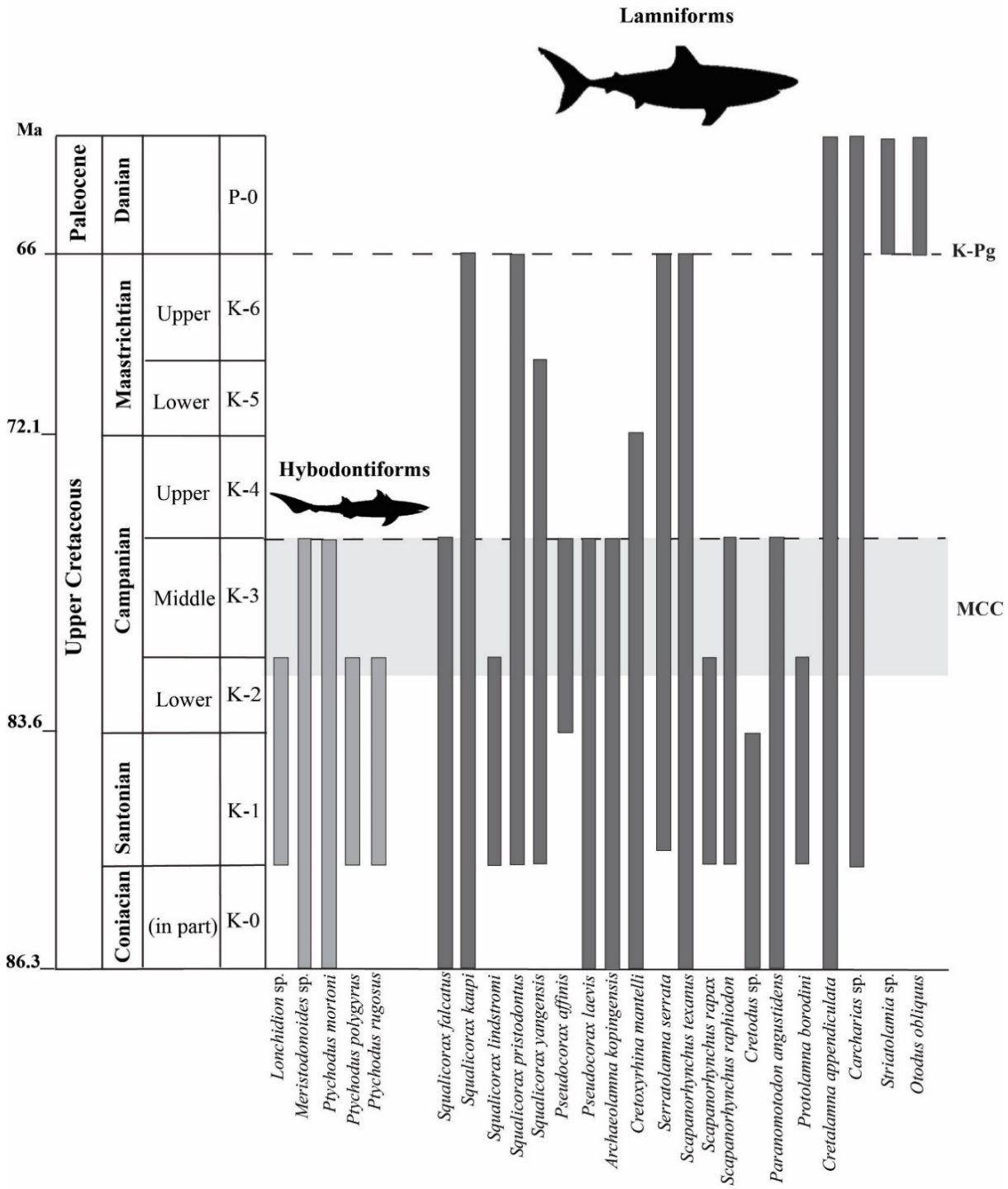

Fig. 7. Stratigraphic occurrences of Late Cretaceous lamniforms and hybodontiforms from northern Gulf of Mexico. Singleton taxa are omitted. Occurrence data by species are available in Appendix Table S3.

4.3. Extinction and origination patterns

We calculated three different extinction and origination values (i.e., extinction and origination percentages, proportional and per-capita rates) for each time-bin at the specific level. Diversity data without singletons for both shark groups at the specific and generic levels is available in Table S5.

4.3.1. Lamniforms

In a total of 25 species of lamniform sharks through the eight time-bins, extinction percentages (Table 2) were highest in the middle Campanian and late Maastrichtian (54.55% and 80.00%, respectively). Proportional and per-capita extinction values (Fig. 8) were nearly zero during the Santonian, but they increased from early to middle Campanian and peaked in the middle Campanian ($P_{E m.y.}$ = 0.56 and $P_{O m.y.}$ = 0.43). Extinction values decreased in the late Campanian and remain low throughout the early Maastrichtian. The highest extinction values ($P_{E m.y.}$ = 1.10 and $P_{O m.y.}$ = 0.67) occurred in the late Maastrichtian and recorded the end-Cretaceous mass extinction, although the total occurrence count was considerably low (n = 34; Table 1). Lamniforms lost a total of nine species in the MCC but only lost four species at the end-Maastrichtian. Concerning diversity loss, the MCC may have been a bigger event than the end-Cretaceous mass extinction for lamniforms.

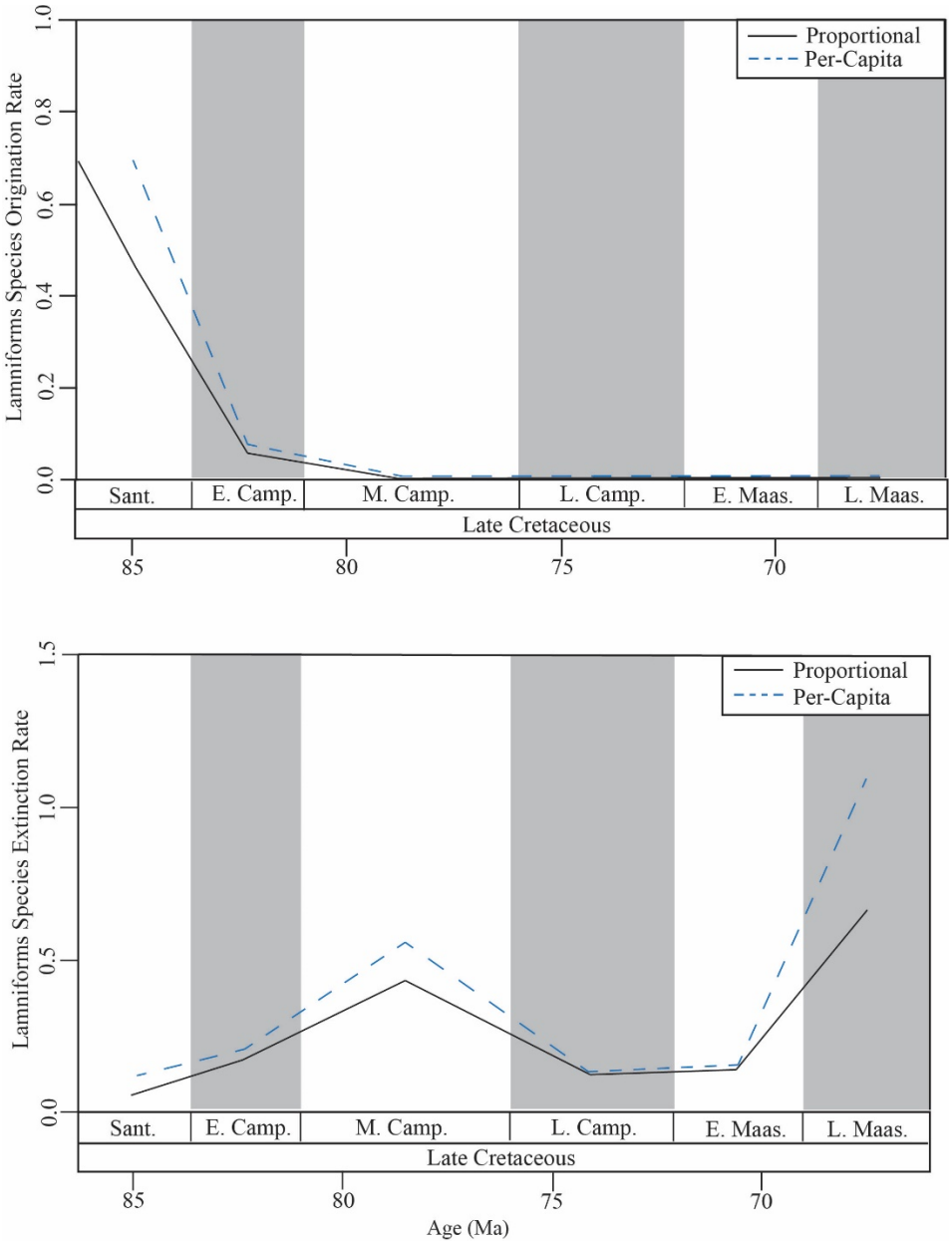

Fig. 8. Proportional and per-capita extinction and origination rates for Late Cretaceous lamniform sharks in northern Gulf of Mexico. **Top**: Lamniform originations. **Bottom**: Lamniform extinctions. Raw data are available in Table 2.

Origination rates indicate that the highest lamniform origination rates occurred in the Santonian (Fig. 8; Table 2). Origination percentages fall from 47.06% in the Santonian to 5.88% in the early Campanian and, finally, to 0.00% from the middle Campanian to late Maastrichtian.

Proportional and per-capita rates show originations declined from the early Campanian to late Maastrichtian, where they remained nearly zero until after the end-Cretaceous mass extinction. Other extinction and origination estimations (e.g., Three-timer, Corrected Three-timer, Gap-filler, Second-for-third) are in Table S9.

Table 2. Data on species counts and extinctions and originations for lamniforms. Lazarus taxa were included. Singleton taxa were omitted. Sums of species occurrences, originations, and extinctions are calculated from time-bins K-1 through K-6.

Stratigraphic Unit	Species Counts			Standing Diversity	Per Capita Rate		Percentage	
	Occ.	Orig.	Ext.		Orig.	Ext.	Ori.	Ext.
Danian (P-0)	4	—	—	—	—	—	—	—
L. Maastrichtian (K-6)	5	0	4	1.33	0.00	1.10	0.00%	80.00%
E. Maastrichtian (K-5)	6	0	1	0.32	0.00	0.15	0.00%	16.67%
L. Campanian (K-4)	6	0	1	0.26	0.00	0.13	0.00%	16.67%
M. Campanian (K-3)	11	0	6	1.20	0.00	0.56	0.00%	54.55%
E. Campanian (K-2)	17	1	3	1.54	0.07	0.21	5.88%	17.65%
Santonian (K-1)	17	8	1	3.33	0.69	0.12	47.06%	5.88%
Coniacian (K-0)	9	—	—	—	—	—	—	—
Sum (K1-K6)	62	9	16		—	—	—	—
Mean	10.3	1.5	2.7		0.09	0.27	8.83%	31.90%
SD	5.6	3.2	2.1		0.19	0.24	18.90%	28.88%

4.3.2. Hybodontiforms

High extinction rates and low origination rates characterize hybodontiform diversity patterns from the Santonian to late Maastrichtian (Table 3). Proportional and per-capita extinction values showed an increasing trend beginning in the Santonian and continued to increase through the middle Campanian (Fig. 9). During the Santonian and early Campanian, origination rates decline before reaching zero by the end of the middle Campanian. Extinction percentages of hybodontiforms were the highest in the early and middle Campanian (60.00% and 100.00%, respectively) (Table 3). Proportional extinction values were also highest in the early Campanian to middle Campanian (0.6 and 1.00, respectively). As indicated by species

occurrence data and extinction rates, most hybodontiforms disappeared by the end of the middle Campanian, at least regionally. Origination rates could not be calculated for any time-bin following the middle Campanian to the end-Maastrichtian due to the lack of new occurrences in the fossil record. Proportional and per-capita rates displayed the highest origination values in the Santonian ($P_{Em.y.}$ = 0.60 and q = 0.92) before dropping to 0.0 in the early Campanian through the late Maastrichtian. Per-capita rates indicate a much faster decline in originations than proportional values.

For species occurrence data, all five hybodontiform species disappear from the regional fossil record by the beginning of the late Campanian (Table 3; Fig. 7). Although extinction rates are highest in the middle Campanian, the greatest species loss occurred in the early Campanian (n = 5 in the early Campanian and n = 2 in the middle Campanian), indicating an earlier diversity decline than lamniforms.

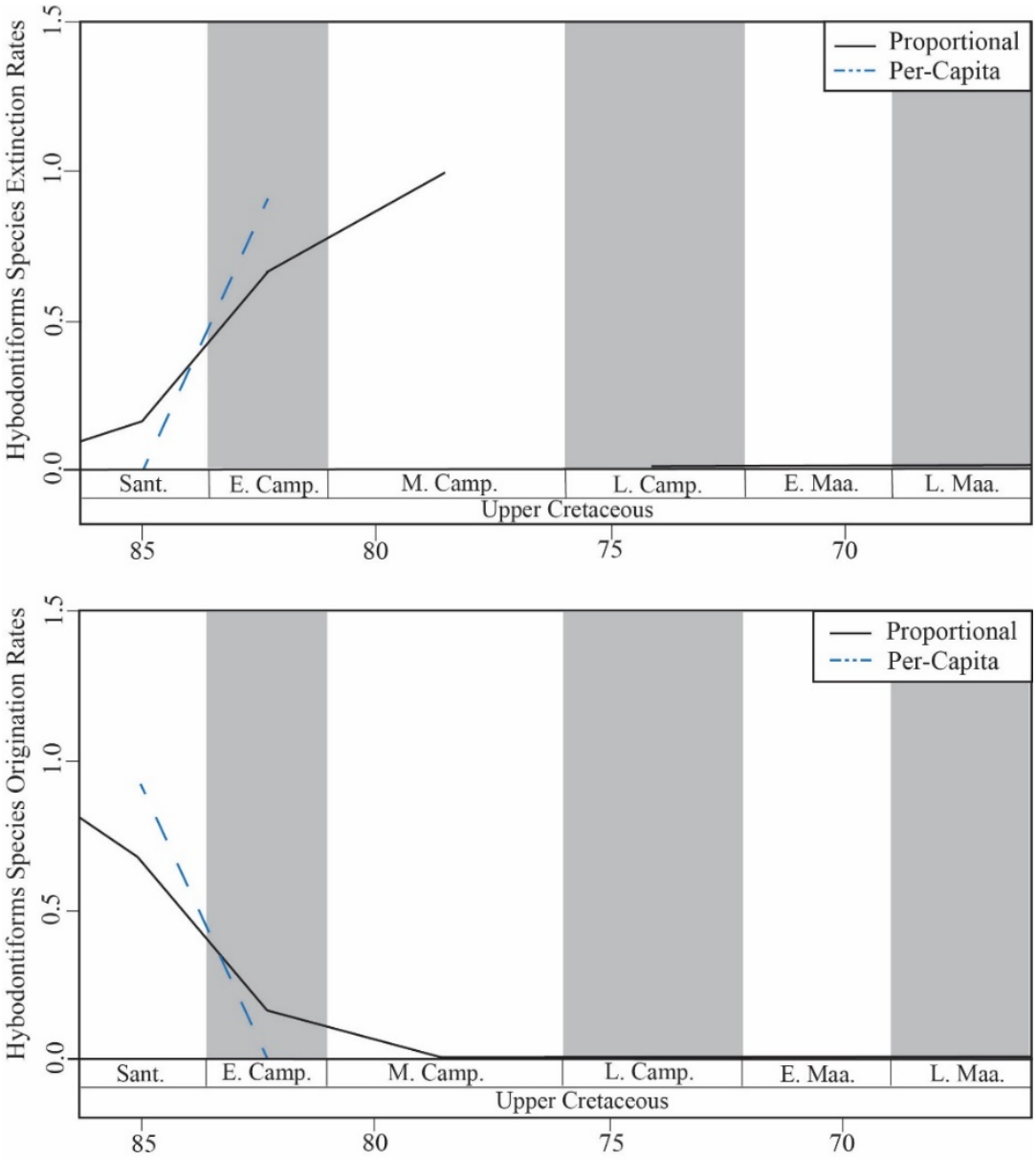

Fig. 9. Proportional and per-capita extinction and origination rates for Late Cretaceous hybodontiforms in northern Gulf of Mexico. **Top**: Hybodontiform originations. **Bottom**: Hybodontiform extinctions. Raw data are available in Table 3.

Table 3. Data on species counts and extinctions and originations for hybodontiforms. Lazarus taxa were included. Singleton taxa were omitted. Sums of species occurrences, originations, and extinctions are calculated from time-bins K-1 through K-6.

Stratigraphic Unit	Species Counts			Standing Diversity	Per Capita Rate		Percentage	
	Occ.	Orig.	Ext.		Orig.	Ext.	Ori.	Ext.
Danian (P-0)	0	0	0	—	—	—	—	—
L. Maastrichtian (K-6)	0	0	0	0.0	—	—	—	—
E. Maastrichtian (K-5)	0	0	0	0.0	—	—	—	—
L. Campanian (K-4)	0	0	0	0.0	—	—	—	—
M. Campanian (K-3)	2	0	2	0.4	0.00	0.00	0.00%	100.00%
E. Campanian (K-2)	5	0	3	1.2	0.00	0.92	0.00%	60.00%
Santonian (K-1)	5	3	0	1.1	0.92	0.00	60.00%	0.00%
Coniacian (K-0)	2	?	—	—	—	—	—	—
Sum (K1-K6)	12	3	5		—	—	—	—
Mean	2.00	0.50	0.83		0.31	0.31	0.00	0.00
SD	2.45	1.22	1.33		0.53	0.53	—	—

4.4. Trends in key marine paleoenvironmental variables

In this study, we draw on global proxy datasets for statistical analyses. However, we discuss how regional trends compare to global trends, which substantiates the use of global datasets (see section 5.3).

Global $\delta^{18}O$ from marine fossil shells shows rapid short-term and long-term fluctuations across the last 20 million years of the Late Cretaceous (Prokoph et al., 2008; reported in ‰ vs. SMOW). $\delta^{18}O$ ratios are a commonly used proxy for sea surface temperature (e.g., Moriya et al., 2003; Taylor et al., 2021). We averaged $\delta^{18}O$ ratios for each time-bin duration (Fig. 10). On average, from the Santonian to early Campanian, $\delta^{18}O$ values decreased by approximately 0.3 ‰ from -2.4 ‰ to -2.7 ‰. Starting in the early to middle Campanian, $\delta^{18}O$ values increase by 1.2 ‰ and remain relatively constant through the late Campanian. The last major fluctuation in $\delta^{18}O$ values occurred from the early to late Maastrichtian when values increased from -1.4 ‰ to -0.5 ‰. The greatest change in $\delta^{18}O$ occurred from the early to middle Campanian (an increase of 1.2

‰). However, long-term trends show the greatest fluctuation in $\delta^{18}O$ values occurred from the early Campanian to late Maastrichtian (an increase of approximately 2.1 ‰). These long- and short-term trends show the transition from 'hot greenhouse' conditions to 'cool greenhouse' conditions (Linnert et al., 2014; 2017).

$\delta^{13}C$ measurements taken from marine fossil shells ($\delta^{13}C_{carb}$ (‰ vs. PDB)) are interpreted here as a proxy for marine productivity, which sustains higher trophic levels in marine ecosystems. We also averaged $\delta^{13}C_{carb}$ ratios for each time-bin duration (Fig. 10). Although $\delta^{13}C_{carb}$ is a proxy for sea level (e.g., Liu, 2009), Figure 10 shows that during global transgressions (e.g., middle to late Campanian), $\delta^{13}C_{carb}$ values did not correspondingly increase. Therefore, here, we interpret $\delta^{13}C_{carb}$ (Prokoph et al., 2008) as a proxy for primary marine productivity (e.g., Locklair et al., 2011). Relative to the early Campanian to end-Maastrichtian, Santonian $\delta^{13}C_{carb}$ values (on average approximately 2.5 ‰) were high. This is likely due to Ocean Anoxic Event (OAE) III, which took place across the Coniacian-Santonian boundary (e.g., Wagreich, 2009; Locklair et al., 2011). $\delta^{13}C_{carb}$ increased to about 2.8 ‰ in the early Campanian. From the middle Campanian to late Maastrichtian, $\delta^{13}C_{carb}$ values continuously declined.

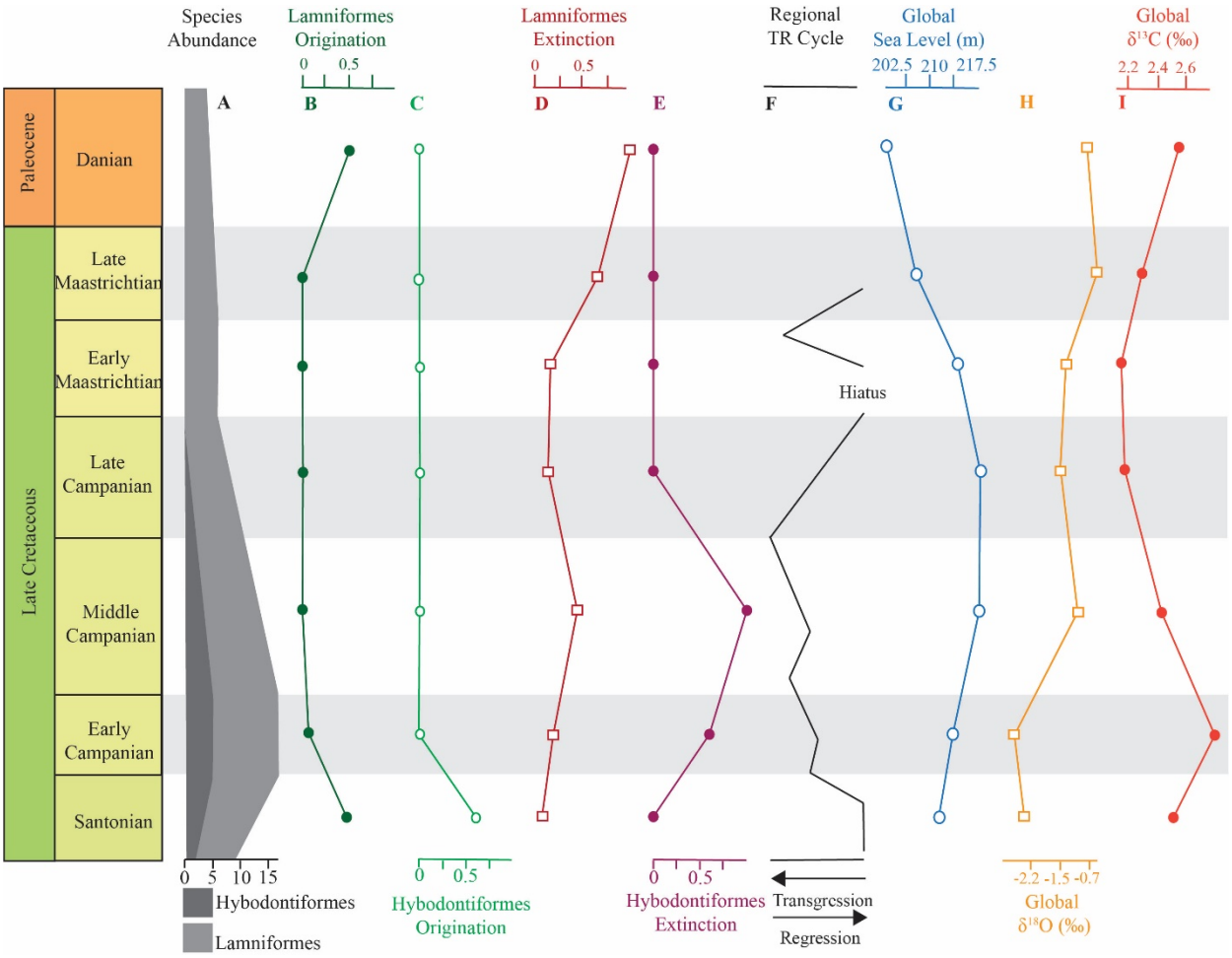

Fig. 10. Profiles of species abundance (A), origination rates (B-C), extinction rates (D-E) and geochemical proxies (G-I) across the Late Cretaceous. Regional transgressive-regressive cycles (F) from the Late Cretaceous northeastern Gulf of Mexico are modified from Mancini and Puckett (2002). Global temperate zone sea level estimates (m) are modified from Haq (2014). Global marine carbonate $\delta^{18}O$ (‰ vs. SMOW) and $\delta^{13}C_{carb}$ (‰ vs. PDB) are from fossil shells (averages were computed for each time interval using data from Prokoph et al. (2008)). Mean values and 95% confidence intervals (CIs) of parameters shown in Fig. 10 are available in Table S14.

4.5. Correlation of paleoenvironments with shark diversity

We investigated to what extent environmental changes, including changing sea levels (Mancini and Puckett, 2002; Haq, 2014), ocean temperatures, and primary marine productivity (Prokoph et al., 2008), affected species abundance and extinction and origination rates (Fig. 10). Pearson's linear, Spearman's rho rank, and Kendall's tau rank correlation tests correlated proportional (hybodontiforms + lamniforms) and per-capita (hybodontiforms + lamniforms) extinction and origination rates with $\delta^{18}O$, $\delta^{13}C_{carb}$, global sea level (m)

For proportional extinction and origination correlations, Pearson's *r* showed significant correlations between species abundance and $\delta^{18}O$ ($P = 0.04$) and extinction and $\delta^{18}O$ ($P = 0.03$) (Table 4). Correlation coefficients indicate a high negative correlation between species abundance and $\delta^{18}O$ ($r = -0.72$) and a high positive correlation between extinction and $\delta^{18}O$ ($r = 0.75$). Spearman's ρ shows significant correlations between extinction and $\delta^{18}O$ ($P = 0.01$) and origination and $\delta^{13}C_{carb}$ ($P = 0.05$). Both correlation coefficients between extinction and $\delta^{18}O$ and origination and $\delta^{13}C_{carb}$ indicate high positive correlations ($\rho = 0.83$ and $\rho = 0.74$, respectively). Kendall's τ shows only a single significant correlation between extinction and $\delta^{18}O$ ($P = 0.01$) with a high positive correlation coefficient ($\tau = 0.71$).

Table 4. Correlation tests (Pearson's *r*, Spearman's ρ, and Kendall's τ) for possible controlling parameters and Late Cretaceous lamniform and hybodontiform proportional extinction and origination rates. Upper triangles show *P*-values. Lower triangles show correlation coefficients. Asterisks (*) indicate significant correlations ($P < 0.05$).

Pearson's *r*

	$\delta^{18}O$	$\delta^{13}C$	Species Abundance	Origination	Extinction	Global Sea Level
$\delta^{18}O$		0.1751	0.0460*	0.1631	0.0317*	0.5781
$\delta^{13}C$	–0.5316		0.0609	0.3575	0.7788	0.4860
Species Abundance	–0.7155	0.6849		0.7792	0.2595	0.5291
Origination (All)	–0.5444	0.3768	0.1189		0.6623	0.2831
Extinction (All)	0.7511	0.1191	–0.4532	–0.1842		0.0908
Global Sea Level	–0.2334	–0.2900	0.2630	–0.4336	–0.6348	

Spearman's ρ

	$\delta^{18}O$	$\delta^{13}C$	Species Abundance	Origination	Extinction	Global Sea Level
$\delta^{18}O$		0.3894	0.0609	0.1738	0.0130*	0.5821
$\delta^{13}C$	–0.3571		0.4450	0.0571*	0.7930	0.2162
Species Abundance	–0.6989	0.3133		0.6095	0.1841	0.3250
Origination (All)	–0.5491	0.7407	0.2133		0.3905	0.1429
Extinction (All)	0.8333	0.1191	–0.5302	–0.3576		0.4279
Global Sea Level	–0.2381	–0.5000	0.3976	–0.5874	–0.3333	

Kendall's τ

	$\delta^{18}O$	$\delta^{13}C$	Species Abundance	Origination	Extinction	Global Sea Level
$\delta^{18}O$		0.3223	0.0723	0.1161	0.0133*	0.8046
$\delta^{13}C$	–0.2857		0.4411	0.0633	1.0000	0.2160
Species Abundance	–0.5189	0.2224		0.5532	0.1234	0.3044
Origination (All)	–0.4536	0.5361	0.1712		0.3173	0.0633
Extinction (All)	0.7143	0.0000	–0.4448	–0.2887		0.4579
Global Sea Level	–0.0714	–0.3571	0.2965	–0.5361	–0.2143	

For per-capita extinction and origination correlations, pearson's *r* indicated a significant correlation and high negative coefficient of correlation between species abundance and $\delta^{18}O$ ($P = 0.04$; $r = -0.07$) (Table 5). Kendall's τ showed a significant correlation and a high positive

coefficient of correlation between origination and species abundance ($P = 0.04$; $\tau = 0.74$) (Table 5). Spearman's ρ identified no significant correlations between any of the parameters.

Table 5. Correlation tests (Pearson's r, Spearman's ρ, and Kendall's τ) for possible controlling parameters and Late Cretaceous lamniform and hybodontiform per-capita extinction and origination rates. Upper triangles show P-values. Lower triangles show correlation coefficients. Asterisks (*) indicate significant correlations ($P < 0.05$).

Pearson's *r*

	$\delta^{18}O$	$\delta^{13}C$	Species Abundance	Origination	Extinction	Global Sea Level
$\delta^{18}O$		0.1751	0.0456*	0.2419	0.1304	0.5781
$\delta^{13}C$	–0.5316		0.0609	0.5447	0.9997	0.4860
Species Abundance	–0.7155	0.6849		0.1649	0.5370	0.5291
Origination (All)	–0.5658	0.3139	0.6471		0.4287	0.5574
Extinction (All)	0.6885	0.0002	–0.3195	–0.4026		0.3515
Global Sea Level	–0.2334	–0.2900	0.2630	–0.3045	–0.4661	

Spearman's *ρ*

	$\delta^{18}O$	$\delta^{13}C$	Species Abundance	Origination	Extinction	Global Sea Level
$\delta^{18}O$		0.3894	0.0609	0.1333	0.1556	0.5821
$\delta^{13}C$	–0.3571		0.4450	0.1333	0.9597	0.2162
Species Abundance	–0.6989	0.3133		0.1333	0.4333	0.3250
Origination (All)	–0.7775	0.7775	0.8356		0.3333	0.4000
Extinction (All)	0.6571	0.0286	–0.4414	–0.5071		0.6583
Global Sea Level	–0.2381	–0.5000	0.3976	–0.4395	–0.2571	

Kendall's *τ*

	$\delta^{18}O$	$\delta^{13}C$	Species Abundance	Origination	Extinction	Global Sea Level
$\delta^{18}O$		0.3223	0.0723	0.0896	0.0909	0.8046
$\delta^{13}C$	–0.2857		0.4410	0.0896	0.8510	0.2160
Species Abundance	–0.5189	0.2224		0.0371*	0.3130	0.3044
Origination (All)	–0.6025	0.6025	0.7396		0.2253	0.2253
Extinction (All)	0.6000	–0.0667	–0.3581	–0.4303		0.5730
Global Sea Level	–0.0714	–0.3571	0.2965	–0.4303	–0.2000	

Principal component analysis (PCA) visualizes multivariate data for the strength of correlation and the direction of correlation among variables grouped based on our established time-bins. The input parameters for PCA are the same as those for the correlation analyses. Proportional and per-capita rates are separately analyzed. The loading and eigenvalue results of proportional PCA are in Figs. S1 and S2. Results of per-capita data PCA are available in Figures S3 through S7 and Tables S12 and S13.

Based on PCA using lamniform proportional extinction and origination datasets (Table S10), proportional origination rates and $\delta^{13}C_{carb}$ were aligned when $\delta^{13}C_{carb}$ was highest during the Coniacian, Santonian, and early Campanian (Fig. 11). The highest extinction rates for lamniforms occurred in the late Maastrichtian to Danian, representing the K-Pg mass extinction. The extinction vector is aligned negatively with global sea level and positively aligned with $\delta^{18}O$, indicating extinctions are highest during low sea level and decreased sea surface temperatures. These data indicate a possible link between unique paleoenvironmental conditions and lamniform species abundance and originations. Further, rising global sea levels may control lamniform extinctions in the late Maastrichtian to Danian.

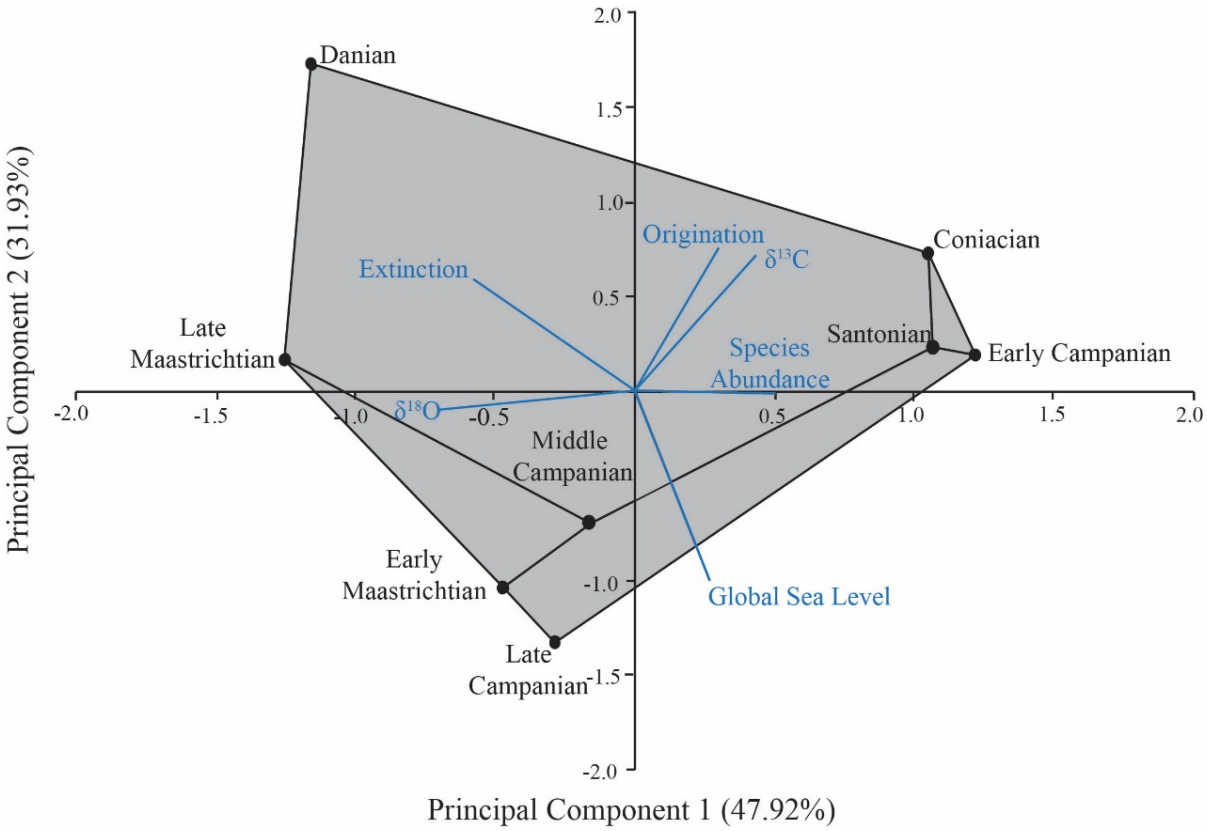

Fig. 11. Principal component analysis for the relationships between lamniform diversity (proportional extinction and origination, species abundance) and paleoenvironmental controls ($\delta^{18}O$, $\delta^{13}C_{carb}$, and global sea level). Raw data are available in Table S10.

The results of PCA using hybodontiform proportional extinction and origination datasets (Fig. 12; Table S11) indicated a positive correlation between $\delta^{13}C_{carb}$ and species abundance and that they were relatively high during the Coniacian, Santonian, and early Campanian. Species abundance and $\delta^{13}C_{carb}$ are correlated negatively with $\delta^{18}O$. The origination rates are correlated negatively with $\delta^{18}O$; origination rates are relatively high in the Coniacian to Santonian when sea surface temperatures were warmer. In the early to middle Campanian, hybodontiform extinction and global sea level vectors showed a positive correlation. Like lamniforms, these data indicate a possible link between unique paleoenvironmental conditions and hybodontiform species

abundance and originations. There is a strong link between hybodontiform extinction and global sea levels in the middle Campanian, which suggest that global sea levels were a controlling factor.

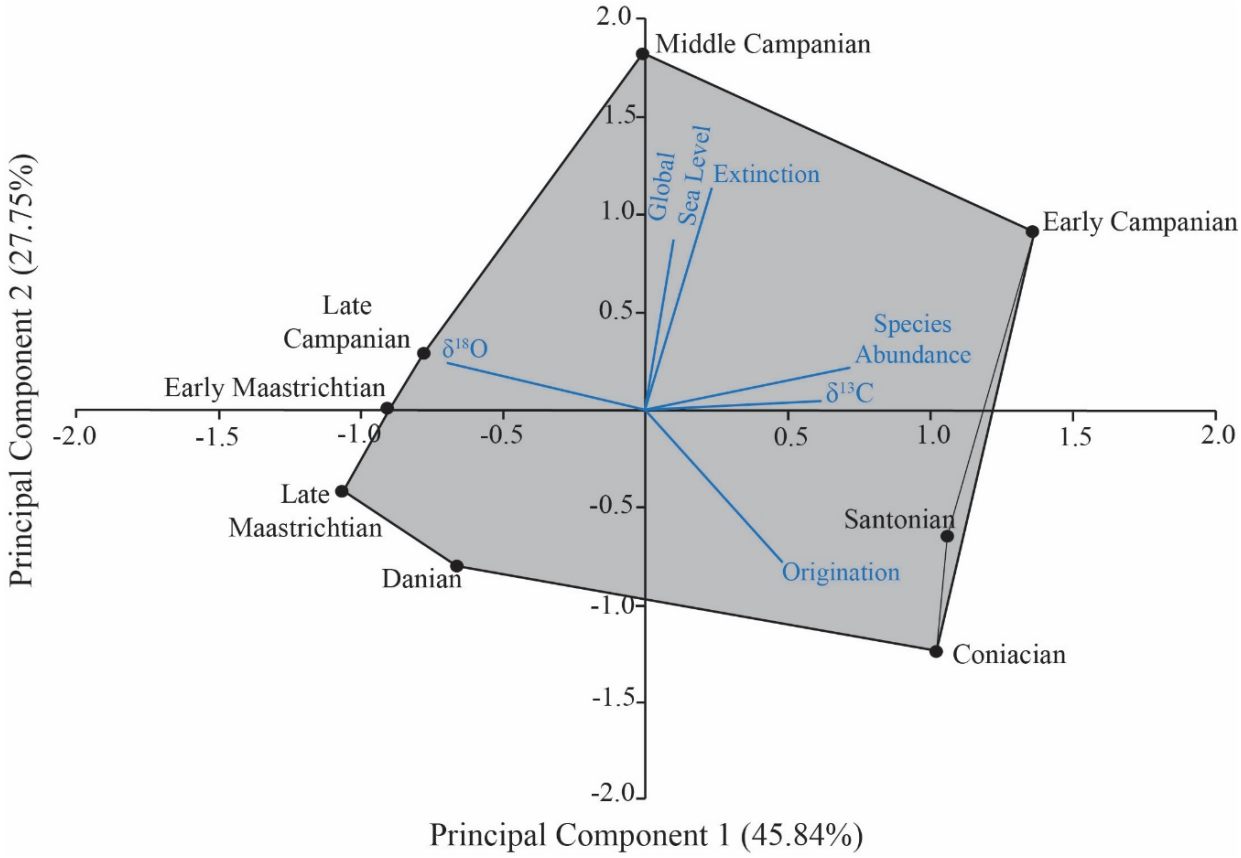

Fig. 12. Principal component analysis for the relationships between hybodontiform diversity (proportional extinction and origination, species abundance) and paleoenvironmental controls ($\delta^{18}O$, $\delta^{13}C_{carb}$, and global sea level). Raw data are available in Table S11.

5. DISCUSSION

The near-continuous deposition of Upper Cretaceous strata provides an ideal place to study marine vertebrate diversity. Sharks are one of the most abundant marine fossils from Late Cretaceous units because they continuously shed their teeth throughout their lifetimes. Their teeth are highly mineralized tissues, which are ideal materials for preservation. However, there are important questions regarding preservation and sampling biases in the fossil record to address when analyzing diversity data. The fossil record is by default incomplete because of sampling, preservational, and sedimentological biases (Alroy, 2010c). Therefore, diversity analyses cannot avoid the possibilities of inconsistencies or incompleteness in the fossil record. Examining sampling variations and estimated species richness (e.g., SQS) is one way of addressing such potential biases (e.g., Ikejiri et al., 2020). To address potential biases from the rock record, we used six different parameters to assess sampling variations in terms of geologic unit duration, the number of fossil sites, unit thickness, and rock volume are compared (Table S4). The duration of each formation (or members) has the strongest tendency to be correlated with unit thickness and the number of localities. A possible limitation may be the number of fossil sites (i.e., localities) for each unit. The highest number of localities is in the Mooreville Chalk Formation that spans the lower to middle Campanian. Other formations range in the number of localities from six to twenty-five (Table S4). Our results are consistent with previously published investigations into sampling bias and the fossil record of Alabama (e.g., Ikejiri et al., 2013, 2020). Coupled with rarefaction and SQS, correlations confirm that Alabama's Late Cretaceous shark fossil record is a reasonably robust sample size.

Differentiating between the relative amplitudes of diversity events (e.g., species abundance in individual time intervals) is an important issue to address when investigating

diversity data. High species abundance occurred in the Santonian and early Campanian and relatively low abundance in the middle and late Campanian. Do the Santonian and early Campanian show unusually high abundance, or do the middle and late Campanian show unusually low abundance? SQS both shark groups and two subsampled groups (lamniforms and hybodontiforms, separately) coupled with extinction and origination rates, the Santonian and early Campanian had very high species abundance. Moreover, the high diversity of sharks and marine vertebrate fauna in the Santonian-Campanian interval is consistent with other diversity studies (e.g., Guinot, 2013; Ikejiri et al., 2020). Those studies also indicate declining or relatively low species diversity in the middle to late Campanian intervals.

Data on species counts and various taxonomic rates of Late Cretaceous hybodontiform and lamniform sharks in the northern Gulf of Mexico exhibit different extinction paths toward the K-Pg mass extinction (Figs. 7-9). Specifically, the former group shows the earlier timing of diversity loss with a significantly higher magnitude of extinction in the area (based on 95% CI: Table 3). The latter group shows later timing and a lower magnitude of loss (Table 2). The combined diversity declines of Late Cretaceous hybodontiform and lamniform sharks from the Santonian to middle Campanian (starting about 12 Myr before the K-Pg boundary) likely reflect the Middle Campanian Crisis (MCC; first coined by Ikejiri et al., 2020). Below, we will discuss the following: (1) key characteristics of the MCC including the timing, duration, paleogeographic range, and possible victims; (2) how those diversity patterns provide insight into shark extinction pathways towards the K-Pg boundary; and (3) possible paleoenvironmental controls.

5.1. Key features of the Middle Campanian Crisis (MCC)

The MCC can play a key role in facilitating the final stage of faunal turnover from hybodontiforms to lamniforms in the northern Gulf of Mexico. The MCC marks the beginning of a time interval of relatively high extinction rates for both hybodontiforms and lamniforms. Our results show complete species loss of hybodontiforms and about half the species of lamniforms (nine out of twenty species) (Fig. 7; Table 2; Table 3). Hybodontiform extinction rates began to rise during the Santonian and early Campanian and peaked in the middle Campanian (Fig. 9; Table 3), indicating a diversity decline for the group had a duration of approximately 10.6 million years. Lamniform extinctions, however, did not begin to increase until the early Campanian (Fig. 8; Table 2), lasting 7.6 million years in duration. The magnitude of lamniform extinction peaks during the middle Campanian ($P_{Em.y.}$ = 0.43 and q = 0.56; Table 2 and Table S5) are about half those of hybodontiforms ($P_{Em.y.}$ = 1.00 and q = 0.00; Table 3 and Table S5). The offset in timing and magnitude of shark extinctions suggests that the MCC was not an instantaneous event but a prolonged diversity loss (possibly over 8.9 Myr of the entire Campanian interval) that disproportionally affected the already declining hybodontiforms. Lamniforms had been undergoing multiple radiation events across the Cretaceous, however, during the MCC lamniform diversity significantly declined. While the MCC removed competition in the form of hybodontiforms, it also stunted the trend of lamniform taxonomic radiation. Despite high extinction rates and low origination rates (Fig. 8), lamniforms remained the dominant shark taxon throughout the Late Cretaceous and into the Paleocene.

The MCC has a considerable loss of sharks and other marine vertebrates in the northeastern Gulf of Mexico, but was the diversity loss event regional or global? At the regional scale, no hybodontiforms have been found in the upper Campanian to Maastrichtian strata in

Alabama (Fig. 9; Tables 2 and 3). The absence from those local formations does not necessarily indicate global-scale hybodontiform extinction during the middle Campanian. Hybodontiform fossils (i.e., generally, isolated teeth) from post-middle Campanian strata are rare but are reported from the central Gulf of Mexico (e.g., Texas) and the Atlantic coastal area (e.g., Maryland, New Jersey) in North America (Welton and Farrish, 1993; Rees and Underwood, 2002; Becker et al., 2006) (Table 6). Post-MCC occurrences of lamniform species are also scarce. Possible MCC survivors outside the Gulf of Mexico include *Archaeolamna kopingenesis* from Campanian-Maastrichtian strata of southernmost South America (Schroeter et al., 2014) and *Protolamna borodini* from Campanian-Maastrichtian strata of New Jersey (Cappetta and Case, 1975). Based on the last global occurrences of MCC victims (Table 6), there is an apparent northward concentration in the post-MCC time, which suggests the northern Gulf of Mexico was no longer a suitable habitat for those sharks (Fig. 13). Since robust records of lamniforms and other marine vertebrate fossils (e.g., bony fishes, mosasaurs, sea turtles) from upper Campanian-Maastrichtian strata in Alabama are known (Ikejiri et al., 2013, 2020), the disappearance of all hybodontiform and some lamniform species represents a real phenomenon in this area. To further investigate extinction patterns of hybodontiforms, an analysis of spatiotemporal fossil distributions across other paleogeographic regions will be needed.

Table 6. Determining the magnitude of the Middle Campanian Crisis for lamniform and hybodontiform sharks based on the fossil record of the northern Gulf of Mexico. The latest, post-middle Campanian stratigraphic and geographic occurrences are shown below. 'Age' indicates the latest known global occurrence. 'Locality' lists states if in the U.S. 'MCC Magnitude.' indicates if the fossil occurrence is restricted in Alabama.

Taxa	Age	Locality	MCC Magnitude	References
Hybodontiforms				
Ptychodus mortoni	K-3	AL, GA	Global	This study; Hamm 2020
Ptychodus mammillaris (s)	K-3	AL	Global	This study; Ikejiri et al., 2020
Ptychodus polygryus	K-2	AL	Global	Ikejiri et al., 2013; Hamm and Harrell, 2013
Ptychodus rugosus	K-2	AL	Global	This study; Hamm, 2020
Ptychodus whipplei (s)	K-2	AL	Global	This study; Ikejiri et al., 2020
Meristodonoides multiplicatus	K-3	AL, MS	Global (?)	Ikejiri et al., 2013; Cicimurri et al., 2014
Lonchidion cristatum	K-2	AL, MS	Global	Cappetta and Case, 1975; Cicimurri et al., 2014
Lamniforms				
Squalicorax falcatus	K-3(?)	AL	Global	This study; Applegate, 1970; Shimada and Cicimurri, 2006
Squalicorax lindstromi	K-4	NJ	Global(?)	Callahan et al., 2014
Pseudocorax affinis	K-5	NJ, NC	Local	Case and Cappetta, 2004; Case et al., 2017
Pseudocorax laevis	K-3	AL	Global	This study
Archaeolamna kopingensis	K-4 or 5	NJ, NC	Local (?)	Cappetta and Case, 1975; Case, 1979; Callahan et al., 2014
Scapanorhynchus rapax	K-5	Syria, Morocco	Local	Bardet et al., 2000; Cappetta et al, 2014
Scapanorhynchus raphiodon	K-3	AL	Global	Applegate, 1970; Ikejiri et al., 2013; This study
Paranomotodon angustidens	K-4	NJ, TX	Global	Cappetta and Case, 1975; Welton and Farish, 1993; Callahan et al., 2014
Protolamna borodini	K-4 or 5	NC, NJ	Local (?)	Cappetta and Case 1975; Callahan et al., 2014

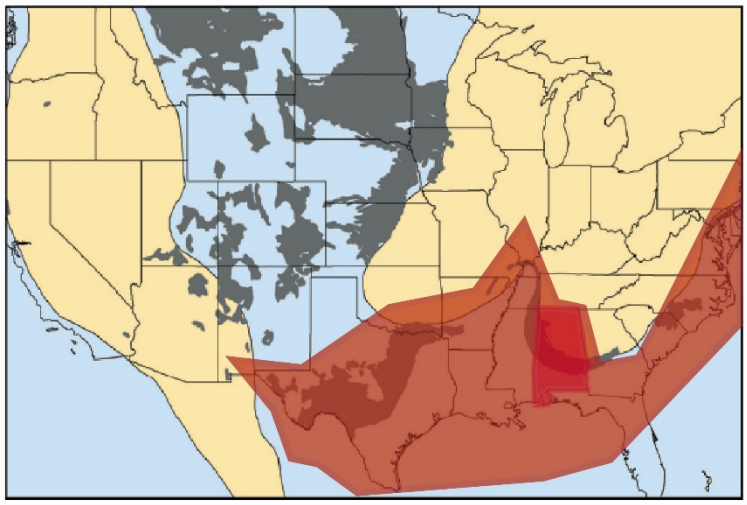

Fig. 13. Paleogeographic map of Santonian North America and the hypothetical range of the MCC based on Table 4. The gray color indicates surface-exposed outcrops of the Upper Cretaceous strata. Light tan indicates Late Cretaceous landmass. Alabama is highlighted in dark red.

Changing marine paleoenvironments (esp., sea levels, sea surface temperatures, and primary marine productivity) across the Late Cretaceous can play an important role in characterizing the MCC. During the K-1 and K-2 intervals, sea surface temperatures and primary marine productivity were relatively high, but those conditions started changing by the K-3. Rising regional and global sea levels, declining sea surface temperatures, and decreasing primary marine productivity characterize the K-3 interval (Fig. 14). By the Maastrichtian, local and global sea levels were regressing while sea surface temperatures and primary marine productivity continued to decline. Thus, the Campanian was a time of long-term environmental transitions compared to the conditions leading up to the K-Pg boundary, which show no long-term changes (Fig. 14). Precisely how these transitioning marine environmental conditions affected Late Cretaceous shark diversity across the MCC remains an important question. We will further discuss the relationships between key paleoenvironmental changes and shark diversity below.

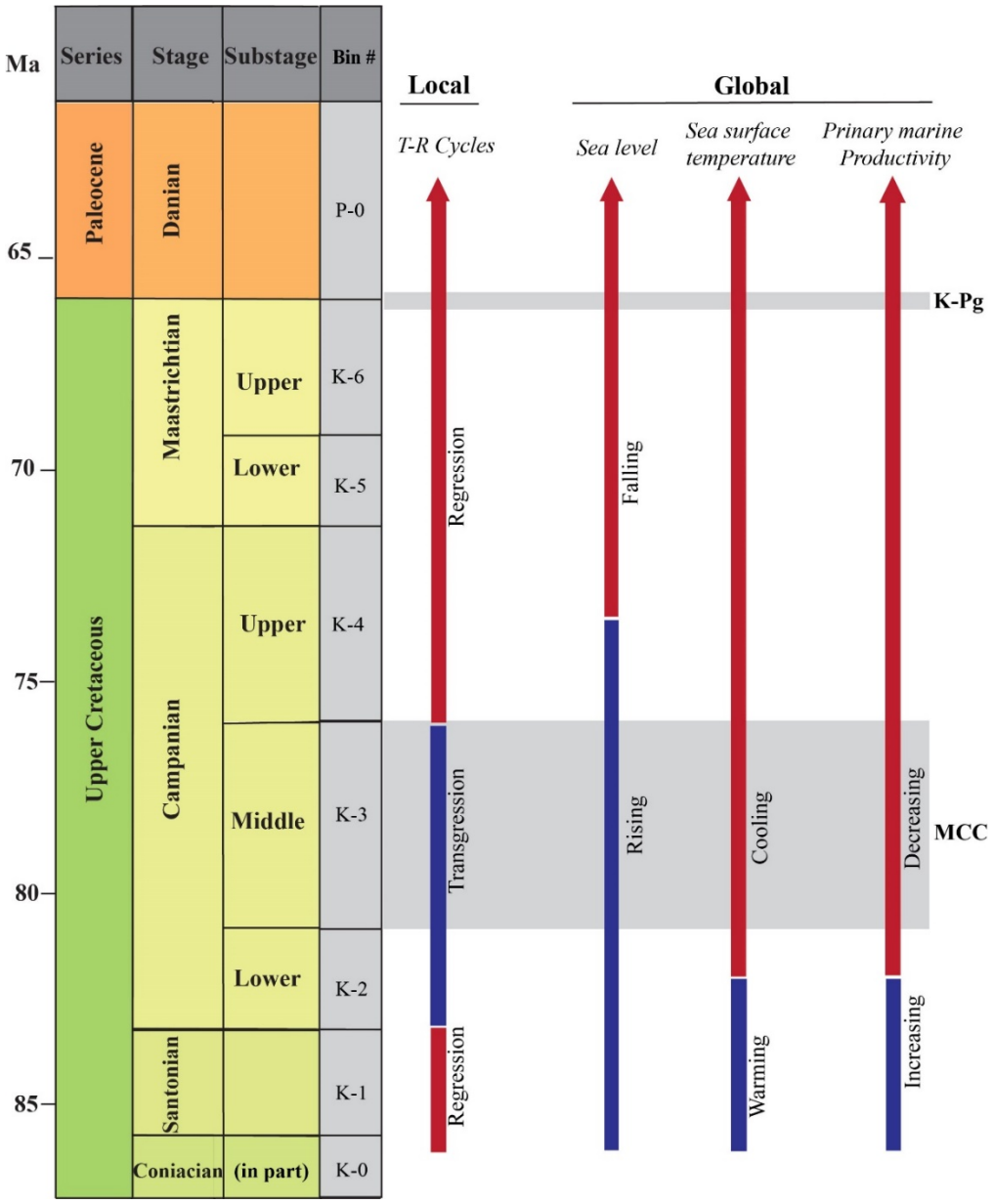

Fig. 14. Characterization of paleoenvironmental conditions (sea level, sea surface temperature, and marine productivity) during the Middle Campanian Crisis. Local sea level transgression and regression data were modified from Mancini and Puckett (2002). Global sea levels are modified from Haq (2014). Global $\delta^{18}O$ and $\delta^{13}C_{carb}$ are modified from Prokoph et al. (2008). Abbreviations of key paleoecological events: K-Pg: Cretaceous—Paleogene mass extinction; MCC: Middle Campanian Crisis.

5.2. Impacts of the MCC on the K-Pg extinction

Bazzi et al. (2018) found that, unlike other marine predators, shark disparity across the K-Pg boundary remained nearly static. Arguably, the MCC was a bigger event for shark species loss than the K-Pg event (Table 1), which may, in part, explain the static disparity observed across the K-Pg. The MCC could have selectively removed certain species that possessed morphologically unfavorable dentition (e.g., blunt, transversely wide-tooth crown of *Ptychodus*) as paleoenvironmental transitions made survival increasingly difficult for sharks. Initial MCC extinctions of hybodontiforms and lamniforms may have been triggered by changing paleoenvironments, which then may have led to the selective removal of tooth morphologies that were not adaptable to those changing conditions. However, to confirm this hypothesis, investigations into shark morphological selectivity and prey availability across the MCC are needed.

5.3. Regional vs. global paleoenvironmental trends

Global $\delta^{18}O$ and $\delta^{13}C_{carb}$ curves can be useful to determine the possible impact of sea surface temperature and primary marine productivity changes on extinctions of Late Cretaceous sharks. Continuous oxygen and carbon isotope data are not available from the Coniacian to Maastrichtian in the northern Gulf of Mexico, and global datasets are substituted for statistical analyses. Existing regional isotope records (Liu, 2009; Meyer et al., 2018), which contain temporal gaps, were compared to global datasets for validation that global records are a reasonable approximation for regional conditions (Fig. 15). While absolute values can differ between the two datasets, both regional and global oxygen and carbon ratios are positively correlated, substantiating the use of global datasets for examining paleoenvironmental controls in our study region.

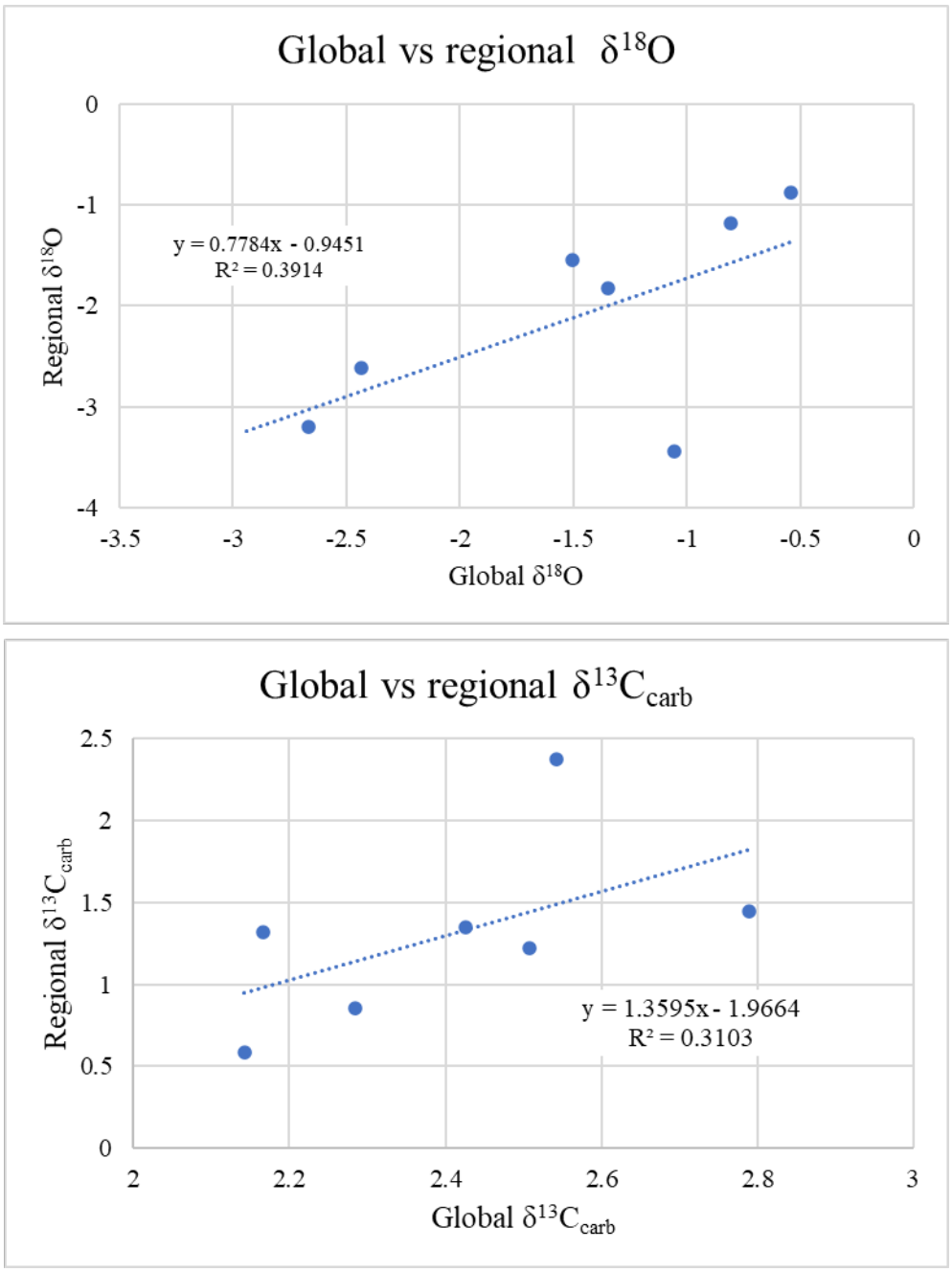

Fig. 15. Comparison of regional versus global $\delta^{18}O$ and $\delta^{13}C_{carb}$ of marine carbonates. The seven dots represent time-intervals from the Santonian (K-1) to Danian (P-0). Global data are from Prokoph et al. (2008) and regional data are from Liu (2009), and Meyer et al. (2018). **Top**: Regional versus global $\delta^{18}O$ isotope data. **Bottom**: Regional versus global $\delta^{13}C_{carb}$ isotope data.

Sea surface temperature changes based on fluctuations in $\delta^{18}O$ across the Upper Cretaceous strata of Alabama correspond with the global Late Cretaceous transition from 'hot greenhouse' to 'cool greenhouse' conditions (Linnert et al., 2014, 2017). Globally, the Santonian-Campanian boundary is recognized by a negative $\delta^{18}O$ excursion marking a thermal-maximum event around 83.8 Ma (e.g., Liu, 2009) (Fig. 10). Regionally, sea surface temperatures reached highs around 28°C to 31°C during the thermal maximum, fell by 6 to 7°C across the late Santonian to early middle Campanian (Liu, 2009), and continued to decline across the Campanian-Maastrichtian (Linnert et al., 2014). Regional and global $\delta^{18}O$ ratios exhibit the same pattern across the Santonian-Campanian intervals (Liu 2009; Prokoph et al., 2008). Following the early Campanian, global oxygen isotope ratios showed a steady increase toward the end-Maastrichtian, which indicates an overall cooling trend. This cooling trend is consistent with other regional studies (Fig. 17; e.g., Linnert et al., 2014, 2017; Meyer et al., 2018).

Late Cretaceous $\delta^{13}C_{carb}$ data from Alabama and Mississippi are also positively correlated with global curves (Fig. 15). The global data indicate relatively high values from the Santonian to early Campanian (Fig. 10). Those high carbon isotope ratios may result from Oceanic Anoxia Event III (OAE III) across the Coniacian-Santonian boundary and the thermal maximum across the Santonian-Campanian. Higher primary marine productivity under warming conditions could have led to the increased burial of organic carbon associated with OAE's (e.g., Liu, 2005). From the middle Campanian to early Maastrichtian $\delta^{13}C_{carb}$ continuously decreased towards the end-Cretaceous.

A regional flooding event occurred around 0.8 Ma following the thermal maximum, and sea levels remained relatively high through the middle Campanian (Liu, 2009). Locally, this transgression is reflected in the sharp lithological change from more sandy units in the Santonian

Eutaw Formation to more chalk- or marl- rich units such as the lower Campanian Mooreville Chalk Formation and middle to upper Campanian Demopolis Chalk (Table S1). Global sea level estimates also display an overall rising trend across the Santonian-Campanian boundary (Haq, 2014; Fig. 10). Globally and regionally, sea levels continued to increase across the early and middle Campanian intervals before reaching it peaked at the middle to late Campanian transition (e.g., Mancini and Puckett 2002, 2005). Following this relatively high sea level sequence in the middle to late Campanian, estimates show a steady sea-level fall across the Maastrichtian into the Paleocene regionally and globally.

5.4. Influence of sea level change on shark diversity

As suggested by the depositional environments, lamniforms likely had a broader habitat range than hybodontiforms, which may explain their contrasting relationships with sea level. In the Late Cretaceous fossil record of the northern Gulf of Mexico, hybodontiform teeth are found more consistently in the sand- or silt-rich marine sedimentary units (e.g., the Eutaw Formation) that represent shallow-water depositional settings (Table S1). However, lamniform fossils are found in both sand- and silt-rich strata and in chalk- or marl-rich formations (e.g., the Mooreville Chalk, Demopolis Chalk) that represent off-shore marine environments. Hybodontiform and lamniform fossils have been found from the same fossil sites in the shallower marine environments of the Coniacian to early Campanian (e.g., AGr-43 in western Alabama; Ciampaglio et al., 2013; Ikejiri et al., 2013). Both shallow water and deeper marine environmental settings suggest that Late Cretaceous lamniforms had broader habitat ranges, which would have been advantageous as marine environments fluctuated. As sea levels rise during the early to middle Campanian, habitat changes could disproportionately affect hybodontiforms, which had adapted to shallow-water settings. Lamniforms dominated shark

populations in deeper waters, and that may have further restricted hybodontiform movement. Similarly, the disappearance of some lamniform taxa is linked to falling global sea levels, possibly because regressions would have diminished available habitat on the continental shelf.

The precise effects of changing sea levels on the different habitats of each shark group remains a key question. Holland (2012) found that marine transgressions do not necessarily signal an increase in shallow marine habitats and that such relationships are dependent on the region in question and the starting point of sea-level change. There is no evidence that polar ice caps were present during the Late Cretaceous, and sea levels were generally high. High starting sea levels may not necessarily indicate increasingly large areas of shallow-marine habitats on the continental shelf. Transgressions are also capable of causing the oxygen minimum zone (OMZ) to expand onto the continental shelf (Smith et al., 2001). Rapid sea-level changes, such as those seen across the Late Cretaceous, could have drastically altered available shallow-marine continental shelf habitats while shifting the OMZ onto the continental shelf. Lamniforms could move their habitats away from areas where near-shore environments were unfavorable. Hybodontiforms likely could not change their habitats to escape rising sea levels or an expanding OMZ. Conversely, from the late Campanian through end-Maastrichtian, lamniforms would be faced with diminishing habitats as sea levels continuously fell. To further test this hypothetical scenario, strata- or layer-based data on placement of the OMZ and fossil occurrences across the Middle Campanian will need to be determined.

5.5. Influence of sea surface temperature and primary marine productivity change on shark diversity

Declining sea surface temperatures across the Late Cretaceous can contribute to the diversity loss of both hybodontiforms and lamniforms. However, our data indicate sea surface

temperature decline disproportionately affected lamniforms. In general, increased temperatures supported shark species abundance and hybodontiform originations (Figs. 11 and 12), and decreased temperatures correlated with lamniform extinctions across the K-Pg boundary (Fig. 11). As previously discussed, the Late Cretaceous climate was transitioning from 'hot greenhouse' to 'cool greenhouse' conditions (see section 5.3). Sea surface temperature was warmer during the Santonian and earliest Campanian compared to the middle to late Campanian and Maastrichtian intervals. Relatively warm surface water temperatures may, in part, explain the relatively high species abundance observed in Santonian and early Campanian time-bins. Relatively low species abundance from early to middle Campanian could result from a dramatic drop in sea surface temperatures (Figs. 10 and 15). Temperature is not correlated with shark extinctions, but our correlation data indicates a possible link between temperature and shark species abundance and originations. Lamniform originations have previously been correlated positively with sea surface temperatures (e.g., Condamine et al., 2019). The transition to cooler global conditions can explain the decline in originations and species abundance following the MCC.

High sea surface temperatures can be a stimulant for primary marine productivity, which provides energy in ecosystems that are passed on to higher trophic levels (i.e., sharks). There is a positive correlation between lamniform originations and hybodontiform species abundance with increased primary marine productivity (Figs. 11 and 12). However, increased productivity may lead to an increase in organic-carbon burial that, along with rising sea levels, could shift or expand the (OMZ) and produce oceanic anoxic conditions (e.g., Jarvis et al., 1988; Freymueller et al., 2019). One such event, known as Oceanic Anoxic Event III (OAE III), occurred across the Coniacian-Santonian boundary. OAE III is known to be a prolonged (at least 7 Myr in duration)

paleogeographically restricted event in the Gulf of Mexico and Atlantic Ocean (Buchs et al., 2018). Subaerial volcanism and subsequent movement of the Caribbean plate triggered the shoaling of waters between the Pacific and early Atlantic oceans. This shoaling would have slowed the flow of oxygen-rich waters from the Pacific into the proto-Caribbean and Atlantic seas (Buchs et al., 2018). Liu (2005) describes OAE III as a Type II OAE that occurred during the early phase of sea-level rise, which resulted in large portions of coastal plains becoming inundated. Coastal inundation allowed for the trapping of carbon in lagoons and estuaries but did not lead to the formation of black shales that are typically characteristic of OAEs (Liu, 2005). Following OAE III, primary marine productivity declined (Fig. 14) across the early Campanian to end-Maastrichtian. While increased primary marine productivity supported high shark species abundance and originations initially, the onset of OAE III combined with a transitioning global climate triggered paleoenvironmental conditions that are unfavorable for the evolution of new species following the MCC.

5.6. Paleoecological implications

The exploitation of food resources from different trophic levels, particularly lower trophic levels, may have disproportionately hindered hybodontiforms. Declining primary marine productivity would have affected lower trophic levels (e.g., invertebrates) before higher trophic groups (e.g., fish, marine reptiles, etc.). Researchers have suggested hybodontiforms were benthic carnivores because they generally possess unique morphologies that exhibit low-crowned, crushing-type surfaces (Maisey, 1982; Fischer, 2008; Rees and Underwood, 2008). Hybodontiform diets were specialized to macroinvertebrates, such as crustaceans and mollusks (durophages), to small fish (macrophages) (Klimley, 2013). Lamniforms had a broader, generalist range of prey types that included macroinvertebrates, small to large fishes, and marine

reptiles (macrophages) (see Schwimmer et al., 1997; Everhart, 2004; Kubo et al., 2012; Schwimmer et al., 2015). Taking advantage of multiple feeding strategies (i.e., specialists vs. generalists) may have enabled some species to survive longer into the MCC than others (e.g., *Ptychodus polygyrus* vs. *Meristodonoides multiplicatus*; Fig. 7). Hybodontiform teeth are typically specialized for a specific type of prey, and they may not have been able to adapt their diets. Those hybodontiforms with less specialized diets (e.g., *Meristodonoides multiplicatus*) could compete with other sharks for resources. Ultimately, the specialized diets and habitat restrictions of hybodontiforms further strained declining populations as sea levels fluctuated and marine productivity fell.

Cooling sea surface temperatures during the Late Cretaceous may also have interfered with hybodontiform and lamniform thermoregulation in such a way that it was detrimental to their ability to survive in the northern Gulf of Mexico. With few exceptions, most modern and prehistoric sharks are ectothermic, meaning that their internal body temperatures are dependent on the ambient waters surrounding them (Table S3; Klimley, 2013; Schlaff et al., 2014). Researchers suggest hybodontiforms were likely ectothermic because of their near-shore habitat and being slow swimmers that may have been capable of short bursts of rapid speed (Maisey, 2012; Klimley, 2013). Sea surface temperatures may have become too low for hybodontiform habitability locally or globally (Fig. 10; Table S3). Lamniforms may have faced a similar challenge. Condamine et al. (2019) found that Cenozoic lamniform originations declined as sea temperatures dropped. It is unlikely that many Mesozoic lamniform sharks were endothermic. Ferron (2017) has, however, suggested that endothermy may have evolved as early as the Late Cretaceous in such shark species as *Cretoxyrhina mantelli* and *Cretalamna appendiculata*. Endothermic lamniforms would have been capable of withstanding sea surface temperature

fluctuations more successfully than ectothermic species. Differences in thermoregulation may explain why certain hybodontiform and lamniform species became extinct or migrated out of the northern Gulf of Mexico and possibly why lamniform originations remained near zero after the MCC.

6. CONCLUSIONS

Hybodontiform and lamniform extinctions were highest in the middle Campanian and are consistent with the timing of the Middle Campanian Crisis (MCC). High global and regional sea levels, warm sea surface temperatures, and decreasing primary marine productivity characterize the MCC, resulting in higher extinction rates and lower originations. For early modern shark evolution, the MCC could be a significant late-stage event in the process of faunal turnover from the end of the hybodontiform lineage to the beginnings of lamniform shark radiation in the Cenozoic. Species that regionally disappeared potentially migrated to other areas such as the Atlantic seaboard, likely due to unsuitable conditions in the Gulf of Mexico and the closing of the Western Interior Seaway. Species with post-middle Campanian occurrences outside the northern Gulf of Mexico area did not survive more than a few million years past the MCC. Coupled with the paleogeographic distribution of post-middle Campanian occurrences, the MCC was likely to have been an ecosystem-wide regional diversity crisis. The number of species lost during the MCC was greater than that of the K-Pg extinction, which indicates, at least regionally, the MCC may have been the greater diversity crisis. Concerning the paleoenvironmental parameters tested here, the main contributing factor to shark decline was global sea level. However, the effects of sea-level changes affected each group differently. Differences in habitat ranges and dietary preferences likely contributed to the differences in timing and magnitude of the two distinct extinction pathways towards the K-Pg.

REFERENCES

Alegret, L., Thomas, E., and Lohmann, K.C., 2011. End-Cretaceous marine mass extinction not caused by productivity collapse. Proceedings of the National Academy of Sciences 109, 728-732.

Alroy, J., 2008. Dynamics of origination and extinction in the marine fossil record. Proceedings of the National Academy of Sciences 105, 11536-11542.

Alroy, J., 2010a. The shifting balance of diversity among major marine animal groups. Science 329, 1191-1193.

Alroy, J., 2010b. Shareholder Quorum Subsampling. https://bio.mq.edu.au/~jalroy/SQS-3-3.R, accessed 15 December 2020.

Alroy, J., 2010c. Geographical, environmental and intrinsic biotic controls on Phanerozoic marine divarication. Palaeontology 53, 1211-1235.

Alroy, J., 2014. Accurate and precise estimates of origination and extinction rates. Paleobiology 40, 347-397.

Alroy, J., 2015. A more precise speciation and extinction rate estimator. Paleobiology 41, 633-639.

Alroy, J., 2017a. Effects of habitat disturbance on tropical biodiversity. Proceedings of the National Academy of Sciences 114, 6056-6061.

Alroy, J., 2017b. Multiton subsampling. http://bio.mq.edu.au/~jalroy/multiton.R, accessed 15 December 2020.

Alroy, J., Marshall, C.R., Bambach, R.K., Bezusko, Foote, M., Furish, F.T., Hansen, T.A., Holland, S.M., Ivany, L.C., Jablonski, D., Jacobs, D.K., Jones, D.C., Kosnik, M.A., Lidgard, S., Low, S., Miller, A.I., Novak-Gottshall, P.M., Olszewski, T.D., Patzkowsky, M.E., Raup, D.M., Roy, K., Sepkoski Jr., J.J., Sommers, M.G., Wagner, P.J., and Webber, A., 2001. Effects of sampling standardization on estimates of Phanerozoic marine diversification. Proceedings of the National Academy of Sciences 98, 6261-6266.

Applegate, S.P., 1970. The vertebrate fauna of the Selma Formation of Alabama. Fieldiana: Geology Memoirs 3, 389-432.

Bardet, N., Cappetta, H., Pereda Suberbiola, X., Moutys, M., Al Maleh, A.K., Ahmad, A.M., Khrata, O., and Gannoum, N., 2000. The marine vertebrate faunas from the Late Cretaceous phosphates of Syria. Geological Magazine 137, 269-290.

Bazzi, M., Kear, B.P., Blom, H., Ahlerg, P.E., and Campione, N.E., 2018. Static dental disparity and morphological turnover in shark across the end-Cretaceous mass extinction. Current Biology 28, 2607-2615.

Becker, M.A., Chamberlain, J.A., and Wolf, G.E., 2006. Chrondrichthyans from the Arkadelphia Formation (Upper Cretaceous: Upper Maastrichtian) of Hot Spring County, Arkansas. Journal of Vertebrate Paleontology 80, 700-716.

Belben, R.A., Underwood, C.J., Johanson, Z., and Twitchett, R.J., 2017. Ecological impact of the end-Cretaceous extinction on lamniform sharks. PLoS ONE 12 (6):e0178294. https://doi.org/10.1371/journal.pone.0178294.

Benson, R.B. and Butler, R.J., 2011. Uncovering the diversification history of marine tetrapods: ecology influences the effect of geological sampling biases. In: McGowan, A. J., Smith, A. B. (Eds.), Comparing the geological and fossil records: implications for biodiversity studies: Geological Society, London, Special Publications, 358, pp. 191-208.

Benton, M.J., 2009. The Red Queen and the Court Jester: species diversity and the role of biotic and abiotic factors through time. Science 323, 728-732.

Buchs, D.M., Kerr, A.C., Brims, J.C., Zapata-Villada, J.P., Correa-Restrepo, T., and Rodriguez, G., 2018. Evidence for subaerial development of the Caribbean oceanic plateau in the Late Cretaceous and paleo-environmental implications. Earth and Planetary Science Letters 499, 62-73.

Callahan, W.R., Mehling, C.M., Denton Jr., R.K., and Parris, D.C., 2014. Vertebrate paleontology and stratigraphy of the Late Cretaceous Holmdel Park Site, Monmouth County, New Jersey. Dakoterra 6, 163-169.

Cappetta, H., 1987. Chondrichthyes II. Mesozoic and Cenozoic Elasmobranchii. In: Schultze, H.-P. (Ed.), Handbook of Paleoichthyology, Volume 3B. Gustav Fischer verlag, Stuttgart, p. 193.

Cappetta, H., Bardet, N., Pereda Suberbiola, X., Adnet, S., Akkrim, D., Amalik, M., and Benabdallah, A., 2014. Marine vertebrate faunas from the Maastrichtian phosphates of Benguerir (Ganntour Basin, Morocco): biostratigraphy, paleobiogeography, and paleoecology. Paleogeography, Paleoclimatology, Paleoecology 409, 217-238.

Cappetta, H. and Case, G., 1975.Contribution à l'étude des sélaciens du groupe Monmouth (Campanien -Maestrichtian) du New Jersey.Paleontographica AbteilungA, 151:1-46

Case, G. R., 1979. Cretaceous selachians from the Peedee Formation (Late Maastrichtian) of Duplin County, North Carolina. Brimleyana 2, 77-89.

Case, G.R., Cook, T.D., Sadorf, E.M., and Shannon, K.R., 2017. A late Maastrichtian selachian assemblage from the Peedee Formation of North Carolina, USA. Vertebrate Anatomy Morphology Paleontology 3, 63-80.

Case, G.R. and Schwimmer, D.R., 1988.Late Cretaceous fish from the Blufftown Formation (Campanian) in western Georgia. Journal of Paleontology 62, 290-301.

Ciampagalio, C.N., Cicimurri, D.J., Ebersole, J.A., and Runyon, K.E., 2013. A note on Late Cretaceous fish taxa recovered from stream gravels at site AGr-43 in Greene County, Alabama. Alabama Museum of Natural History Bulletin 31(1), 84-97.

Cicimurri, D.J., Ciampagalio, C.N., and Runyun, K.E., 2014. Late Cretaceous elasmobranchs from the Eutaw Formation at Luxapalila Creek, Lowndes County, Mississippi. PalArc's Journal of Vertebrate Paleontology 11, 1-36.

Clapham, M.E. and Payne, J.L., 2011. Acidification, anoxia, and extinction: a multiple logistic regression analysis of extinction and selectivity during the Middle and Late Permian. Geology 39, 1059-1062.

Condamine, F.L., Romieu, J., and Guinot, G., 2019. Climate cooling and clade competition likely drove the decline of lamniform sharks. Proceedings of the National Academy of Sciences 116, 20584-20590.

Ebersole, J.A. and Dean, L.S., 2013. The history of Late Cretaceous vertebrate research in Alabama. Alabama Museum of Natural History Bulletin 31 (1), 3-45.

Everhart, M.J., 2004. Late Cretaceous interaction between predators and prey. Evidence of feeding by two species of shark on a mosasaur. PalArch's Vertebrate Paleontology 1, 1-7.

Ferron, H.G., 2017. Regional endothermy as a trigger for gigantism in some extinct macropredatory sharks. PLoS ONE 12: e0185185. https://doi.org/10.1371/journal.pone.0185185.

Fischer, J., 2008. Brief synopsis of the hybodont form taxon *Lissodus* Brough, 1935, with remarks on the environment and associated fauna. Freiberger Forschungshefte 528, 1-23.

Foote, M., 1999. Morphological diversity in the evolutionary radiation of Paleozoic and post-Paleozoic crinoids. Paleobiology 25, 1-115.

Foote, M., 2000. Origination and extinction components of taxonomic diversity: general problems. Paleobiology 26, 74-102.

Foote, M. and Miller, A.I., 2007. Principles of Paleontology Third Edition. W.H. Freeman and Company, 345 pp.

Freymueller, N.A., Moore, J.R., and Myers, C.E., 2019. An analysis of the impacts of Cretaceous oceanic anoxic events on global Molluscan diversity dynamics. Paleobiology 45, 280-295.

Good, I.J., 1953. The population frequencies of species and the estimation of population parameters. Biometrika 40, 237-264.

Guinot, G., 2013. Regional to global patterns in Late Cretaceous selachian (Chondrichthyes, Euselachii) diversity. Journal of Vertebrate Paleontology 33, 521-531.

Guinot, G., Adnet, S., and Cappetta, H., 2012. An analytical approach for estimating fossil record and diversification events in sharks, skates and rays. PLoS ONE 7:e44632. https://doi.org/10.1371/journal.prone.0044632.

Hamm, S.A., 2020. Stratigraphic, geographic, and paleoecological distribution of the Late Cretaceous shark genus Ptychodus within the Western Interior Seaway, North America. Bulletin of New Mexico Museum of Natural History and Science 81, pp. 94.

Hamm, S.A. and Harrell Jr., T.L., 2013. A note on the occurrence of *Ptychodus polygyrus* (Ptychodontidae) from the Late Cretaceous of Alabama, with comments on the stratigraphic and geographic distribution of the species. Alabama Museum of Natural History Bulletin 31 (1), 105-113.

Hammer, Ø., Harper, D.A.T., and Ryan, P.D., 2001. PAST: Paleontological statistics software package for education and data analysis. Palaeontologia Electronica 4, 1-9.

Haq, B.U., 2014. Cretaceous eustasy revisited. Global and Planetary Change 113, 44-58.

Hoffman, B.L., Hageman, S.A., and Claycomb, G.D., 2016. Scanning electron microscope examination of the dental enameloid of the Cretaceous durophagous shark *Ptychodus* supports neoselachian classification. Journal of Paleontology 90, 741-762.

Holland, S. M., 2012. Sea level change and the sea of shallow-marine habitat: implications for marine biodiversity. Paleobiology 38, 205-217.

Horton, J.D., 2017. The State Geologic Map Compilation (SGMC) geodatabase of the conterminous United States (ver. 1.1., August 2017): U.S. Geological Survey data release. https://doi.org/10.5066/F7WH2N65.

Ikejiri, T., Ebersole, J.A., Blewitt, H.L., and Ebersole, S.M., 2013. An overview of Late Cretaceous vertebrates from Alabama. Alabama Museum of National History Bulletin 31(1), 46-71.

Ikejiri, T., Lu, Y., and Zhang, B., 2020. Two-step extinction of Late Cretaceous marine vertebrates in northern Gulf of Mexico prolonged biodiversity loss prior to the Chicxulub impact. Scientific Reports 10:4169. https://doi.org/10.1038/s41598-020-61089-w.

Ivanov, A., 2005. Early Permian chondrichthyans of the Middle and South Urals. Revista Brasileira de Paleontologia 8, 127-138.

Jablonski, D. and Raup, D.M., 1995. Selectivity of End-Cretaceous marine bivalve extinctions. Science 268, 389-391.

Jambura, P.L. and Kriwet, J., 2020. Articulated remains of the extinct shark *Ptychodus* (Elasmobranchii, Ptychodontidae) from the Upper Cretaceous of Spain provide insights into gigantism, growth rate and life history of ptychodontid sharks. PLoS ONE 15: e0231544. https://doi.org/10.1371.journal.pone.0231544

Jarvis, I., Carson, G.A., Cooper, M.K.E., Hart, M.B., Leary, P.N., Tocher, B.A., Horne, D., and Rosenfeld, A., 1988. Microfossil assemblages and the Cenomanian-Turonian (Late Cretaceous) oceanic anoxic event. Cretaceous Research 9, 3-103.

Kelley, N. P., Motani, R., Jiang, D., Rieppel, O., and Schmitz, L., 2014. Selective extinction of Triassic marine reptiles during long-term sea-level changes illuminated by seawater strontium isotopes. Paleogeography, Paleoclimatology, Paleoecology 400, 9-16.

Kiessling, W. and Aberhan, M., 2007a. Environmental determinants of marine benthic biodiversity dynamics through Triassic–Jurassic time. Paleobiology 33, 414-434.

Kiessling, W. and Aberhan, M., 2007b. Geographic distribution and extinction risk: lessons from Triassic–Jurassic marine benthic organisms. Journal of Biogeography 34, 1473-1489.

Kiessling, W., Aberhan, M., Brenneis, B., and Wagner, P.J., 2007. Extinction trajectories of benthic organisms across the Triassic—Jurassic boundary. Palaeogeography, Palaeoclimatology, Palaeoecology 244, 201-222.

Klimley, A.P., 2013. The Biology of Sharks and Rays. The University of Chicago Press, Chicago, p. 512.

Kocsis, A.T., Reddin, C.J., Alroy, J., and Kiessling, W., 2019. The R package divDyn for quantifying diversity dynamics using fossil sampling data. Methods in Ecology and Evolution 10, 735-743.

Kriwet, J. and Benton, M.J., 2004. Neoselachian (Chondrichthyes, Elasmobranchii) diversity across the Cretaceous-Tertiary boundary. Palaeogeography, Palaeoclimatology, Palaeoecology 214, 181-194.

Kubo, T., Mitchell, M.T., and Henderson, D.M., 2012. *Albertonectes vanderveldei*, a new elasmosaur (Reptilia, Sauropterygia) from the Upper Cretaceous of Alberta. Journal of Vertebrate Paleontology 32, 557-572.

Linnert, C., Robinson, S.A., Lees, J.A., Brown, P.R., Perez-Rodriguez, I., Petrizzo, M.R., Falzoni, F., Littler, K., Arz, J.A., and Russell, E.E., 2014. Evidence for global cooling in the Late Cretaceous. Nature Communications 5:4194. https://doi.org/10.1038/ncomms5194.

Linnert, C., Robinson, S.A., Lees, J.A., Perez-Rodriguez, I., Jenkyns, H.C., Petrizzo, M.R., Arz, J.A., Brown, P.R., and Falzoni, F., 2017. Did Late Cretaceous cooling trigger the Campanian-Maastrichtian Boundary event? Newsletters on Stratigraphy 51, 145-166.

Liu, K., 2005. Upper Cretaceous sequence stratigraphy, Sea-level fluctuations and Oceanic Anoxic Events 2 and 3, Northeastern Gulf of Mexico. Stratigraphy 2, 147-166.

Liu, K., 2009. Oxygen and carbon isotope analysis of the Mooreville Chalk and late Santonian-Early Campanian Sea level and sea surface temperature changes, northeastern Gulf of Mexico, USA. Cretaceous Research 30, 980-990.

Locklair, R., Sageman, B., and Lerman, A., 2011. Marine carbon burial flux and the carbon isotope record of Late Cretaceous (Coniacian-Santonian) Oceanic Anoxic Event III. Sedimentary Geology 235, 38-49.

Lu, M., Ikejiri, T., and Lu, Y., 2021. A synthesis of the Devonian wildfire record: implications for paleogeography, fossil flora, and paleoclimate. Palaeogeography, Palaeoclimatology, Palaeoecology 571, 110321.

Maisey, J.G., 1982. The anatomy and interrelationships of Mesozoic hybodont sharks. American Museum Novitates 2724, 1-48.

Maisey, J.G., 2012. What is an 'elasmobranch'? The impact of paleontology in understanding elasmobranch phylogeny and evolution. Journal of Fish Biology 80, 918-1951.

Maisey, J.G., Naylor, G. J., and Ward, D. J., 2004. Mesozoic elasmobranch, neoselachian phylogeny and the rise of modern elasmobranch diversity. Mesozoic fishes 3, 17-56.

Mancini, E.A. and Puckett, T.M., 2002. Transgressive-regressive cycles: application to petroleum exploration for hydrocarbons associated with Cretaceous shelf carbonates and coastal and fluvial-deltaic siliciclastics, northeastern Gulf of Mexico. 22nd Annual Gulf Coast Section SEMP Foundation Bob F. Perkins Research Conference, 173-199.

Mancini, E.A. and Puckett, T.M., 2005. Jurassic and Cretaceous transgressive-regressive (T-R) cycles, northern Gulf of Mexico, USA. Stratigraphy 2, 31-48.

Mancini, E.A., Puckett, T.M., and Tew, B.H., 1996. Integrated biostratigraphic and sequence stratigraphic framework for Upper Cretaceous strata of the eastern Gulf Coastal Plain, USA. Cretaceous Research 17, 645-699.

Mancini, E.A., Puckett, T.M., Tew, B.H., and Smith, C.C., 1995. Upper Cretaceous sequence stratigraphy of Mississippi-Alabama area. Gulf Coast Association of Geological Societies Transactions 45, 377-384.

Meyer, K.W., Peterson, S.V., Lohmann, K.C., and Winkelstern, I.Z., 2018. Climate of the Late Cretaceous North American Gulf and Atlantic coasts. Cretaceous Research 89, 160-173.

Moriya, K., Nishi, H., Kawahata, H., Tanabe, K., and Takayanagi, Y., 2003. Demersal habitat of Late Cretaceous ammonoids: evidence from oxygen isotopes for the Campanian (Late Cretaceous) northwestern Pacific thermal structure. Geology 31, 167-170.

Patterson, C., 1966. British wealden sharks. Bulletin of British Museum of Natural History (Geol) 11, 283-350.

Prokoph, A., Shields, G.A., and Veizer, J., 2008. Compilation and time-series analysis of a marine carbonate $\delta^{18}O$, $\delta^{13}C$, $^{87}Sr/^{86}Sr$ and $\delta^{34}S$ database through Earth History. Earth-Science Reviews 87, 113-133.

Raup, D.M., 1991. The future of analytical paleobiology. Short Courses in Paleontology 4, 207-216.

Raymond, D.E., Osborne, W.E., Copeland, C.W., and Neathery, T.L., 1988. Alabama stratigraphy. Geological Survey of Alabama Circular 140, 1-97.

R Core Development Team., 2020. R: a language and environment for statistical computing. Vienna: R Foundation for statistical computing.

Rees, J., 2006. Hybodont sharks from the Middle Jurassic of the Inner Hebrides, Scotland. Transactions of the Royal Society of Edinburgh: Earth Sciences 96, 351-363.

Rees, J. and Underwood, C.J., 2002. The status of the shark genus *Lissodus* Brough, 1935, and the position of nominal *Lissodus* species within the Hybodontoidea (Selachii). Journal of Vertebrate Paleontology 22, 471-479.

Rees, J. and Underwood, C.J., 2008. Hybodont sharks of the English Bathonian and Callovian (Middle Jurassic). Paleontology 51, 117-147.

Schlaff, A.M., Heupel, M.R., and Simpfendorfer, C.A., 2014. Influence of environmental factors on shark and ray movement, behaviour and habitat use: a review. Reviews in Fish Biology and Fisheries 24, 1089-1103.

Schroeter, E.R., Egerton, V.M., Ibiricu, L.M., and Lacovara, K.J., 2014. Lamniform shark teeth from the Late Cretaceous of southernmost South America (Santa Cruz Province, Argentina). PLoS ONE 9: e104800. https://doi.org/10.1371/journal.pone.0104800.

Schwimmer, D.R., Stewart, J.D., and Williams, G.D., 1997. Scavenging by sharks of the genus *Squalicorax* in the Late Cretaceous of North America. Palaois 12, 71-83.

Schwimmer, D.R., Weems, R.E., and Sanders, A.E., 2015. A Late Cretaceous shark coprolite with baby freshwater turtle vertebrae inclusions. Palaios 30, 707-713.

Shimada, K., 2009. The first associated teeth of the Late Cretaceous Anacoracid shark, *Pseudocorax laevis* (Leriche), from the Mooreville Chalk of Alabama. Transactions of the Kansas Academy of Science 112, 164-168.

Shimada, K., 2012. Dentition of Late Cretaceous shark, *Ptychodus mortoni* (Elasmobranchii, Ptychodontidae). Journal of Vertebrate Paleontology 32, 12

Shimada, K. and Hooks III, G.E., 2004. Shark-bitten protostegid turtles from the Upper Cretaceous Mooreville Chalk, Alabama. Journal of Paleontology 78, 205-210.

Shimada, K. and Cicimurri, D.J., 2006. The oldest record of the Late Cretaceous anacoracid shark, *Squalicorax pristodontus* (Agassiz), from the Western Interior, with comments on *Squalicorax* phylogeny. New Mexico Museum of Natural History and Science Bulletin 35, 177-84.

Smith, A.B., Gale, A.S., and Monks, N.E.A., 2001. Sea-level change and rock-record bias in the Cretaceous: a problem for extinction and biodiversity studies. Paleobiology 27, 241-253.

Taylor, L.T., Minzoni, R.T., Suarez, C.A., Gonzalez, L.A., Martin, L.D., Lambert, W.J., Ehret, D.J., and Harrell, T.L., 2021. Oxygen isotopes from the teeth of Cretaceous marine lizards reveal their migration and consumption of freshwater in the Western Interior Seaway, North America. Paleogeography, Paleoclimatology, Paleoecology 573:110406. https://doi.org/10.1016/j.paleo.2021.110406.

Thurmond, J.T. and Jones, D.E., 1981. Fossil vertebrates of Alabama: Tuscaloosa, University of Alabama Press, pp. 244.

Underwood, C.J., 2006. Diversification of the Neoselachii (Chondrichthyes) during the Jurassic and Cretaceous. Paleobiology 32, 215-235.

Wagreich, M., 2009. Coniacian-Santonian oceanic red beds and their link to Oceanic Anoxic Event 3. SEPM Special Publication 91, 235-242.

Welton, B.J. and Farish, R.F., 1993. The collector's guide to fossil sharks and rays from the Cretaceous of Texas. Horton Printing Co., Dallas, Texas.

APPENDIX I

Table S1. Table of lithologic descriptions for Late Cretaceous geologic units in western and central Alabama (Raymond et al., 1988). Asterisks (*) denote members of larger formations.

Geologic Units	Key Lithology
Prairie Bluff Chalk Formation	Bluish-gray firm, sandy, fossiliferous brittle chalk; unconsolidated material is grayish-black silty sandy calcareous glauconitic, fossiliferous clay
Ripley Formation	Light-gray to pale-olive massive, bioturbated, micaceous, glauconitic fine sand, sandy calcareous clay and thin, indurated beds of fossiliferous sandstone
Bluffport Marl Member*	Massive chalky very dark-gray marl, very clayey chalk, and calcareous clay
Demopolis Chalk Formation	Light-gray to medium-light-gray fossiliferous chalk; lower portion of formation consists of thin beds of marly chalk
Arcola Limestone Member*	Two to four beds of light-gray impure dense, brittle fossiliferous limestone with softer marl interbeds
Mooreville Chalk Formation	Yellowish-gray to dark-bluish gray clayey compact fossiliferous chalk and chalky marl; near base of formation includes thin glauconitic and clayey marl beds
Tombigbee Sand Member*	Light-gray massive to weakly bedded, highly glauconitic sand that is somewhat clayey; locally, may include layers of calcareous sandstone and sandy chalk
Eutaw Formation	Light-greenish-gray fine- to medium-grained well-sorted micaceous cross-bedded sand that is fossiliferous and glauconitic in part and contains beds of greenish-gray micaceous, silty clay and medium-dark-gray carbonaceous clay

*Bluffport Marl Member of the Demopolis Chalk Formation
*Arcola Limestone Member of the Mooreville Chalk Formation
*Tombigbee Sand Member of the Eutaw Formation

Table S2. List of institutions housing specimens used in this study.

Abbreviation	Name of Institution
ALMNH	Alabama Museum of Natural History, Tuscaloosa, AL
AMNH	American Museum of Natural History, New York, NY
AUMNH	Auburn University Museum of Natural History, Auburn, AL
CCK	Cretaceous Research Collections at Columbus State University, Columbus, GA
CSU	Columbus State University, Columbus, GA
FHSM	Fort Hays State University Sternberg Museum of Natural History, Hays, KS
FMNH	Field Museum of Natural History, Chicago, IL
GSA	Geological Survey of Alabama, Tuscaloosa, AL
KUVP	University of Kansas Museum of Natural History, Lawrence K,S
MMNH	Mississippi Museum of Natural History, Jackson, MS
MSC	McWane Science Center, Birmingham, AL
RMM	Red Mountain Museum (housed at McWane Science Center), Birmingham, AL
USNM	United States National Museum, Washington D.C.
WSU	Wright State University, Dayton, OH

Table S3. Taxonomic list with stratigraphic occurrences of Late Cretaceous lamniform and hybodontiform sharks from the northern Gulf of Mexico. The symbol 's' next to species names indicates singleton taxa. Age Ranges: Con. = Coniacian; E. Camp. = Early Campanian; M. Camp. = Middle Campanian; L. Camp. = Late Campanian; E. Maa. = Early Maastrichtian; L. Maa. = Late Maastrichtian; Dan. = Danian. Thermoregulation (Thermo): Ecto = Ectomorphic; Meso = Mesothermic. Guild: Macro = Macropredatory; Duro = Durophagous.

Order	Family	Genus	Species	Paleoecology	Thermo	Guild	Stratigraphic Range
Lamniformes	Anacoracidae	*Squalicorax*	*falcatus*	Nektonic carnivore	Ecto	Macro	Con. – M. Camp.
Lamniformes	Anacoracidae	*Squalicorax*	*kaupi*	Nektonic carnivore	Ecto	Macro	Con. – L. Maa.
Lamniformes	Anacoracidae	*Squalicorax*	*lindstromi*	Nektonic carnivore	Ecto	Macro	Sant. – E. Camp.
Lamniformes	Anacoracidae	*Squalicorax*	*pristodontus*	Nektonic carnivore	Ecto	Macro	Sant. – L. Maa.
Lamniformes	Anacoracidae	*Squalicorax*	*yangensis*	Nektonic carnivore	Ecto	Macro	Sant. – E. Maa.
Lamniformes	Anacoracidae	*Pseudocorax*	*affinis*	Nektonic carnivore	Ecto	Macro	E. Camp. – M. Camp.
Lamniformes	Anacoracidae	*Psuedocorax*	*laevis*	Nektonic carnivore	Ecto	Macro	Con. – M. Camp.
Lamniformes	Alopiidae	*Paranomotodon*	*angustidens*	Nektonic carnivore	Ecto	Macro	Con. – M. Camp.
Lamniformes	Archaeolamnidae	*Archaeolamna*	*kopingensis*	Nektonic carnivore	Ecto	Macro	Con. – M. Camp.
Lamniformes	Cretoxyrhinidae	*Cretoxyrhina*	*mantelli*	Nektonic carnivore	Endo?	Macro	Con. – L. Camp.
Lamniformes	Serratolamnidae	*Serratolamna*	*serrata*	Nektonic carnivore	Ecto	Macro	Sant. – L. Maa.
Lamniformes	Eoptolamnidae	*Protolamna*	*borodini*	Nektonic carnivore	Ecto	Macro	Sant. – E. Camp.
Lamniformes	Mitsukurinidae	*Scapanorhynchus*	*texanus*	Nektonic carnivore	Ecto	Macro	Con. – L. Maa.
Lamniformes	Mitsukurinidae	*Scapanorhynchus*	*rapax*	Nektonic carnivore	Ecto	Macro	Sant. – E. Camp.
Lamniformes	Mitsukurinidae	*Scapanorhynchus*	*raphiodon*	Nektonic carnivore	Ecto	Macro	Sant. – M. Camp.
Lamniformes	Odontaspididae	*Carcharias*	sp.	Nektonic carnivore	Ecto	Macro	Sant. – Dan.
Lamniformes	Odontaspididae	*Striatolamia*	sp.	Nektonic carnivore	Ecto	Macro	Dan.
Lamniformes	Otodontidae	*Cretalamna*	*appendiculata*	Nektonic carnivore	Endo?	Macro	Con. – Dan.
Lamniformes	Otodontidae	*Otodus*	*Obliquus*	Nektonic carnivore	Endo?	Macro	Dan.
Lamniformes	Pseudoscapanorh-ynchidae	*Cretodus*	sp.	Nektonic carnivore	Ecto	Macro	Con. – Sant.
Hybodontiformes	Hybodontidae	*Meristodonoides*	*multiplicatus*	Nektonic carnivore	Ecto	Macro. & Duro?	Con. – M. Camp.
Hybodontiformes	Ptychodontidae	*Ptychodus*	*mortoni*	Benthic carnivore	Ecto	Duro	Con. – M. Camp.
Hybodontiformes	Ptychodontidae	*Ptychodus*	*polygyrus*	Benthic carnivore	Ecto	Duro	Sant. – M. Camp.

Hybodontiformes	Ptychodontidae	*Ptychodus*	*rugosus*	Benthic carnivore	Ecto	Duro	Sant. – M. Camp.
Hybodontiformes	Ptychodontidae	*Ptychodus*	*whipplei* (s)	Benthic carnivore	Ecto	Duro	Sant.
Hybodontiformes	Ptychodontidae	*Ptychodus*	*mamillaris* (s)	Benthic carnivore	Ecto	Duro	E. Camp.
Hybodontiformes	Lonchididae	*Lonchidion sp.*	*cristatum*	Benthic carnivore	Ecto	Macro. & Duro?	Sant. – M. Camp.

Table S4. Sampling variation of Late Cretaceous shark fossils from Alabama. **Top**: Raw data of duration, maximum and median rock unit thicknesses, surface area of each unit, county numbers, and locality numbers. The duration is estimated based on the median of the approximate interval for each stratigraphic unit (see Fig. 2 and Table S1). **Below**: Results of Kendall's tau correlation. The upper triangle of numbers is the *p*-values. The lower triangle of numbers is the τ values.

Geologic Unit	Duration (Myr)	Maximum Thickness (m)[a]	Median Thickness (m)[a]	Surface Area (km^2)[b,c]	# Of Localities	# Of Counties	Species Occurrences
Prairie Bluff Chalk Formation	3.5	33.5	16.8	412	6	3	71
Ripley Formation	4.1	76.2	53.3	2,045	6	5	56
Demopolis Chalk Formation	5.4	150.9	73.9	2,476	10	5	41
Mooreville Chalk Formation	4.6	182.9	56.4	2,642	49	9	1170
Eutaw Formation	4.4	121.9	45.7	4,359	25	12	1230

	Duration	Max Thickness	Median Thickness	Surface Area	Localities	Counties	Species Occurrences
Duration		0.050	0.050	0.327	0.197	0.439	0.624
Max Thickness	0.800		0.142	0.624	0.071	0.197	1.000
Median Thickness	0.800	0.600		0.142	0.439	0.796	0.327
Surface Area	-0.400	-0.200	-0.600		0.796	0.796	0.327
Localities	0.527	0.738	0.316	0.105		0.102	0.439
Counties	0.316	0.527	0.105	0.105	0.667		0.197
Species Occurrences	-0.200	0.000	-0.400	0.400	0.316	0.527	

[a] Raymond et al. (1988).
[b] Based on 1:250,000 state map
[c] Ikejiri et al., 2013, 2020

Table S5. Data on origination and extinction rates for both shark groups with and without singletons. Origination (Orig.) and extinction (Ext.) rates represented here were used in Figures 8 and 9 of the main text. Lazarus taxa were included in species occurrence (Occ.) counts. Standard deviations are calculated using n = 6.

Both Shark Groups (with singletons)

Stratigraphic Unit		Species Counts			Standing Diversity	Proportional Rate		Percentage	
		Occ.	Orig.	Ext.		Orig.	Ext.	Orig.	Ext.
Coniacian		11	--	--	--	--	--	--	--
Santonian		23	12	2	5.19	0.52	0.09	47.83%	4.35%
E. Campanian		23	2	7	3.46	0.09	0.30	4.35%	26.10%
M. Campanian		13	0	8	1.60	0.00	0.50	0.00%	61.54%
L. Campanian		6	0	1	0.26	0.00	0.13	0.00%	16.67%
E. Maastrichtian		6	0	1	0.32	0.00	0.14	0.00%	16.67%
L. Maastrichtian		5	0	4	1.33	0.00	0.67	0.00%	80.00%
Danian		4	--	--	--	--	--	--	--
Sum (K1-K6)		76	14	23	--	--	--	--	--
Mean		12.7	2.3	3.8		0.10	0.31	8.70%	34.22%
SD		8.5	4.8	3.2		0.21	0.23	19.25%	29.72%
95%CI	Lower	5.9	–1.5	1.3		0.04	0.05	3.85%	5.94%
	Upper	19.5	6.2	6.4		0.27	0.49	24.10%	58.00%
	Margin of error	6.8	3.8	2.6		0.17	0.19	15.40%	23.78%

Both Shark Groups (without singletons)

Stratigraphic Unit		Species Counts			Standing Diversity	Per Capita Rate		Percentage	
		Occ.	Orig.	Ext.		Orig.	Ext.	Orig.	Ext.
Coniacian		11	--	--	--	--	--	--	--
Santonian		22	11	1	4.44	0.74	0.10	50.00%	4.55%
E. Campanian		22	1	6	2.69	0.06	0.34	4.55%	27.27%
M. Campanian		13	0	8	1.60	0.00	0.69	0.00%	61.54%
L. Campanian		6	0	1	0.26	0.00	0.13	0.00%	16.67%
E. Maastrichtian		6	0	1	0.32	0.00	0.15	0.00%	16.67%
L. Maastrichtian		5	0	4	1.33	0.00	1.10	0.00%	80.00%
Danian		4	--	--	--	--	--	--	--
Sum (K1-K6)		74	12	21		--	--	--	--
Mean		12.3	2.0	3.5		0.13	0.42	9.09%	34.45%
SD		8.0	4.4	3.0		0.30	0.40	20.12%	29.62%
95% CI	Lower	5.9	–1.5	1.1		0.06	0.08	4.02%	5.92%
	Upper	18.7	5.5	5.9		0.37	0.74	25.19%	58.15%
	Margin of error	6.4	3.5	2.4		0.24	0.32	16.10%	23.70%

Table S5 (cont.)

Lamniformes (with singletons)

Stratigraphic Unit		Species Counts			Standing Diversity	Proportional Rate*		Percentage	
		Occ	Orig.	Ext.		Orig.	Ext.	Orig.	Ext.
Coniacian		9	--	--	--	--	--	--	--
Santonian		17	8	1	3.33	0.47	0.06	47.10%	5.88%
E. Campanian		17	1	3	1.54	0.06	0.17	5.88%	17.65%
M. Campanian		11	0	6	1.20	0.00	0.43	0.00%	54.55%
L. Campanian		6	0	1	0.26	0.00	0.13	0.00%	16.67%
E. Maastrichtian		6	0	1	0.32	0.00	0.14	0.00%	16.67%
L. Maastrichtian		5	0	4	1.33	0.00	0.67	0.00%	80.00%
Danian		4	--	--	--	--	--	--	--
Sum (K1-K6)		62	9	16		--	--	--	--
Mean		10.3	1.5	2.7		0.09	0.27	8.83%	31.90%
SD		5.6	3.2	2.1		0.19	0.24	18.90%	28.88%
95% CI	Lower	5.9	–1.1	1.0		0.04	0.05	3.78%	5.77%
	Upper	14.8	4.1	4.3		0.24	0.45	23.95%	55.01%
	Margin of Error	4.5	2.6	1.7		0.15	0.19	15.12%	23.11%

Hybodontiformes (with singletons)

Stratigraphic Unit		Species Counts			Standing Diversity	Proportional Rate*		Percentage	
		Occ.	Orig.	Ext.		Orig.	Ext.	Orig.	Ext.
Coniacian		2	--	--	--	--	--	--	--
Santonian		6	4	1	1.9	0.67	0.17	66.67%	16.67%
E. Campanian		6	1	4	1.5	0.17	0.67	16.67%	66.67%
M. Campanian		2	0	2	0.4	0.00	1.00	0.00%	100.00%
L. Campanian		--	--	--	0.0	--	--	--	--
E. Maastrichtian		--	--	--	0.0	--	--	--	--
L. Maastrichtian		--	--	--	0.0	--	--	--	--
Danian		--	--	--	--	--	--	--	--
Sum (K1-K6)		14	5	7		--	--	--	--
Mean		2.3	0.8	1.2		0.14	0.31		
SD		2.9	1.6	1.6		0.27	0.43		
95% CI	Lower	0.0	–0.4	–0.1		0.05	0.09		
	Upper	4.7	2.1	2.4		0.35	0.65		
	Margin of Error	2.4	1.3	1.3		0.21	0.34		

Table S6. Shareholder Quorum Subsampling (SQS) for species level richness with and without singletons. The quorum (q) was set at 0.2, 0.4, 0.6, and 0.8, respectively with 1000 iterations per q.

Both Shark Groups SQS (without singletons)

Age	0.2	0.4	0.6	0.8
Santonian	1.2	2.5	4.5	7.2
Early Campanian	0.9	2.6	4.3	7.2
Middle Campanian	0.9	2.1	3.6	5.2
Late Campanian	0.6	1.0	1.9	2.8
Early Maastrichtian	0.9	1.0	1.4	2.4
Late Maastrichtian	0.6	1.0	1.5	2.7

Both Shark Groups SQS (with singletons)

Age	0.2	0.4	0.6	0.8
Santonian	1.2	2.5	4.5	7.4
Early Campanian	0.9	2.5	4.2	7.2
Middle Campanian	0.8	2.1	3.6	5.3
Late Campanian	0.6	1.0	1.9	2.7
Early Maastrichtian	0.9	1.1	1.5	2.4
Late Maastrichtian	0.6	1.0	1.6	2.6

Lamniformes SQS (without singletons)

Age	0.2	0.4	0.6	0.8
Santonian	0.8	1.7	3.0	5.0
Early Campanian	0.8	1.9	3.5	5.2
Middle Campanian	0.8	1.8	3.3	4.9
Late Campanian	0.6	1.0	1.9	2.8
Early Maastrichtian	0.9	1.1	1.4	2.4
Late Maastrichtian	0.7	1.0	1.6	2.7

Lamniformes SQS (with singletons)

Age	0.2	0.4	0.6	0.8
Santonian	0.8	1.7	3.0	5.0
Early Campanian	0.8	1.9	3.5	5.2
Middle Campanian	0.8	1.9	3.3	4.8
Late Campanian	0.6	1.0	1.9	2.7
Early Maastrichtian	0.9	1.1	1.4	2.3
Late Maastrichtian	0.6	1.0	1.6	2.7

Table S6 (cont.)

Hybodontiformes (without singletons)

Age	0.2	0.4	0.6	0.8
Santonian	0.5	0.9	1.5	1.6
Early Campanian	0.6	1.0	1.4	1.6
Middle Campanian	0.5	0.5	1.3	--
Late Campanian	--	--	--	--
Early Maastrichtian	--	--	--	--
Late Maastrichtian	--	--	--	--

Hybodontiformes (with singletons)

Age	0.2	0.4	0.6	0.8
Santonian	0.6	1.0	1.6	1.6
Early Campanian	0.6	1.0	1.4	1.6
Middle Campanian	0.5	0.5	1.4	--
Late Campanian	--	--	--	--
Early Maastrichtian	--	--	--	--
Late Maastrichtian	--	--	--	--

Table S7. Shareholder Quorum Subsampling (SQS) for generic level richness with and without singletons. The quorum (q) was set at 0.2, 0.4, 0.6, and 0.8, respectively with 1000 iterations per q.

Both Shark Groups Genera SQS (with singletons)

Age	0.2	0.4	0.6	0.8
Santonian	0.8	2.0	3.3	5.0
Early Campanian	0.7	1.6	2.7	4.2
Middle Campanian	0.7	1.5	2.6	3.7
Late Campanian	0.6	1.0	1.0	1.5
Early Maastrichtian	0.9	1.0	1.0	1.3
Late Maastrichtian	0.6	1.0	1.0	1.5

Both Shark Groups Genera SQS (without singletons)

Age	0.2	0.4	0.6	0.8
Santonian	0.8	2.0	3.2	5.0
Early Campanian	0.7	1.6	2.7	4.2
Middle Campanian	0.7	1.5	2.6	3.8
Late Campanian	0.6	1.0	0.9	1.5
Early Maastrichtian	0.9	1.0	1.0	1.3
Late Maastrichtian	0.6	1.0	1.0	1.5

Table S8. Multiton subsampling (MS) for species and genus level richness for both shark groups with singletons. The target for all time-bins was based on the Early Campanian. The Early Campanian has the most occurrences and, thus, is at least risk for under sampling. The species and generic targets were set at 6 and 4.7, respectively.

Time-bin	Duration (Myr)	MS Species Diversity	MS Genus Diversity
Santonian	2.7	11.58	7.39
Early Campanian	2.6	11.08	6.49
Middle Campanian	5.0	8.58	5.61
Late Campanian	3.9	6.00	3.04
Early Maastrichtian	3.1	4.33	3.01
Late Maastrichtian	3.0	4.28	3.04

Table S9. Extinction and origination metrics for both shark groups and lamniforms and hybodontiforms, respectively, from data excluding singleton taxa. Asterisks (*) indicate extinction and origination rates shown in Figures 8 and 9 of the main text.

Both Sharks Groups (lamniforms + hybodontiforms)

Variable	Symbol[1]	Santonian	Early Camp.	Middle Camp.	Late Camp.	Early Maa.	Late Maa.
Duration in million years		2.7	2.6	5.0	3.9	3.1	3.0
Two-timers (*i*)	t2d	11	21	13	5	5	1
Two-timers (*i*-1)	t2u	21	13	5	5	5	1
Three-timers	t3	10	12	5	4	4	1
Part-timers	tPart	0	0	1	0	0	0
Gap-fillers (*i*-1)	tGFd	--	0	0	2	0	0
Gap-fillers (*i*+2)	tGFu	0	1	1	0	0	--
Singleton taxa	tSing	0	0	0	0	0	0
Originate	tOri	11	1	0	0	0	0
Extinct	tExt	1	6	8	1	1	4
Crosses both boundaries	tThrough	10	15	8	7	6	2
Sampled-in-Bin	divSIB	22	22	13	6	6	5
Corrected sampled-in-bin	divCSIB	21.41	21.41	15.18	5.84	5.84	4.06
Range-through	divRT	22	22	16	8	7	6
Boundary crosser	divBC	11	21	16	8	7	6
Proportional extinction	extProp*	0.05	0.27	0.50	0.13	0.14	0.67
Proportional origination	OriProp	0.50	0.05	0.0	0.0	0.0	0.0
Per-Capita extinction	extPC*	0.09	0.34	0.69	0.13	0.15	1.10
Per-Capita origination	oriPC	0.74	0.06	0.0	0.0	0.0	0.0
Three-timer extinction	ext3t*	0.10	0.56	0.96	0.22	0.22	1.61
Three-timer origination	ori3t	0.74	0.08	0.0	0.22	0.22	0.0
Corrected three-timer extinction	extC3t*	0.10	0.38	0.96	0.22	0.22	--
Corrected three-timer origination	oriC3t	--	0.08	0.0	0.04	0.22	0.0
Gap-filler extinction	extGF*	0.10	0.48	0.69	0.22	0.22	--
Gap-filler origination	oriGF	--	0.08	0.0	-0.18	0.22	0.0
Second-for-third extinction	ext2f3*	0.10	0.48	0.69	0.22	0.22	--
Second-for-third origination	ori2f3	--	0.08	0.0	0.0	0.22	0.0

Table S9 (cont.)

Lamniforms

Variable	Symbol[1]	Santonian	Early Camp.	Middle Camp.	Late Camp.	Early Maa.	Late Maa.
Duration in million years		2.7	2.6	5.0	3.9	3.1	3.0
Two-timers (*i*)	t2d	9	16	11	5	5	1
Two-timers (*i*-1)	t2u	16	11	5	5	5	1
Three-timers	t3	8	10	5	4	4	1
Part-timers	tPart	0	0	1	0	0	0
Gap-fillers (*i*-1)	tGFd	--	0	0	2	0	0
Gap-fillers (*i*+2)	tGFu	0	1	1	0	0	--
Singleton taxa	tSing	0	0	0	0	0	0
Originate	tOri	8	1	0	0	0	0
Extinct	tExt	1	3	6	1	1	4
Crosses both boundaries	tThrough	8	13	8	7	6	2
Sampled-in-Bin	divSIB	17	17	11	6	6	5
Corrected sampled-in-bin	divCSIB	16.48	16.48	12.80	5.82	5.82	4.85
Range-through	divRT	17	17	14	8	7	6
Boundary crosser	divBC	9	16	14	8	7	6
Proportional extinction	extProp*	0.06	0.18	0.43	0.13	0.14	0.67
Proportional origination	OriProp	0.47	0.06	0.0	0.0	0.0	0.0
Per-Capita extinction	extPC*	0.12	0.21	0.56	0.13	0.15	1.10
Per-Capita origination	oriPC	0.69	0.74	0.0	0.0	0.0	0.0
Three-timer extinction	ext3t*	0.12	0.47	0.79	0.22	0.22	1.61
Three-timer origination	ori3t	0.69	0.10	0.0	0.22	0.22	0.0
Corrected three-timer extinction	extC3t*	0.12	0.29	0.79	0.22	0.22	--
Corrected three-timer origination	oriC3t	--	0.10	0.0	0.04	0.22	0.0
Gap-filler extinction	extGF*	0.12	0.37	0.54	0.22	0.22	--
Gap-filler origination	oriGF	--	0.10	0.0	-0.18	0.22	0.0
Second-for-third extinction	ext2f3*	0.12	0.37	0.54	0.22	0.22	--
Second-for-third origination	ori2f3	--	0.10	0.0	0.0	0.22	0.0

Table S9 (cont.)

Hybodontiforms

Variable	Symbol[1]	Santonian	Early Camp.	Middle Camp.	Late Camp.	Early Maa.	Late Maa.
Duration in million years		2.7	2.6	5.0	3.9	3.1	3.0
Two-timers (*i*)	t2d	2	5	2	0	0	0
Two-timers (*i*-1)	t2u	5	2	0	0	0	0
Three-timers	t3	2	2	0	0	0	0
Part-timers	tPart	0	0	0	0	0	0
Gap-fillers (*i*-1)	tGFd	0	0	0	0	0	0
Gap-fillers (*i*+2)	tGFu	0	0	0	0	0	0
Singleton taxa	tSing	0	0	0	0	0	0
Originate	tOri	3	0	0	0	0	0
Extinct	tExt	0	3	2	0	0	0
Crosses both boundaries	tThrough	2	2	0	0	0	0
Sampled-in-Bin	divSIB	5	5	2	0	0	0
Corrected sampled-in-bin	divCSIB	5	5	0	0	0	0
Range-through	divRT	5	5	2	0	0	0
Boundary crosser	divBC	2	5	2	0	0	0
Proportional extinction	extProp*	0.00	0.6	1.00	0.00	0.00	0.00
Proportional origination	OriProp	0.60	0.00	0.00	0.00	0.00	0.00
Per-Capita extinction	extPC*	0.00	0.92	0.00	0.00	0.00	0.00
Per-Capita origination	oriPC	0.92	0.00	0.00	0.00	0.00	0.00
Three-timer extinction	ext3t*	0.00	0.92	0.00	0.00	0.00	0.00
Three-timer origination	ori3t	0.92	0.00	0.00	0.00	0.00	0.00
Corrected three-timer extinction	extC3t*	0.00	0.00	0.00	0.00	0.00	0.00
Corrected three-timer origination	oriC3t	0.00	0.00	0.00	0.00	0.00	0.00
Gap-filler extinction	extGF*	0.00	0.00	0.00	0.00	0.00	0.00
Gap-filler origination	oriGF	0.00	0.00	0.00	0.00	0.00	0.00
Second-for-third extinction	ext2f3*	0.00	0.00	0.00	0.00	0.00	0.00
Second-for-third origination	ori2f3	0.00	0.00	0.00	0.00	0.00	0.00

Table S10. Results of principal component analysis for comparing possible controls on lamniform diversity dynamics using proportional extinction and origination metrics. Figure 11 of the main text shows graphical representations of the results below.

Summary

PC	Eigenvalue	% Variance
1	2.8751	47.92%
2	1.9157	31.93%
3	0.9400	15.67%
4	0.1694	2.82%
5	0.0973	1.62%
6	0.0025	0.04%

Loadings

	PC 1	PC 2	PC 3	PC 4	PC 5	PC 6
$\delta^{18}O$	–0.568	–0.068	0.205	0.044	0.491	0.623
$\delta^{13}C$	0.339	0.462	0.484	0.421	–0.303	0.409
Species	0.503	–0.006	0.477	–0.381	0.596	–0.142
Origination	0.238	0.480	–0.617	0.288	0.496	0.061
Extinction	–0.457	0.378	0.335	0.312	0.169	–0.641
Global Sea Level	0.210	–0.639	0.059	0.704	0.196	–0.102

Scores

	PC 1	PC 2	PC 3	PC 4	PC 5	PC 6
Danian	–1.1605	1.7355	0.1065	0.4682	–0.0583	–0.9233
Late Maastrichtian	–1.2620	0.1708	0.2550	–0.9880	–0.1516	0.9955
Early Maastrichtian	–0.4651	–1.0292	–0.6114	–0.8227	–0.5446	0.6958
Late Campanian	–0.2866	–1.3334	–0.5573	0.5156	–0.4720	–1.6827
Middle Campanian	–0.1654	–0.7014	–0.9141	1.4718	1.4064	0.7685
Early Campanian	1.2207	0.1927	1.5390	0.0583	–1.4897	0.0824
Santonian	1.0690	0.2306	0.0938	–1.4573	1.4913	–0.7560
Coniacian	1.0498	0.7345	–1.7397	0.7542	–0.1816	0.8199

Table S11. Results of principal component analysis for comparing possible controls on hybodontiform diversity dynamics using proportional extinction and origination metrics. Figure 12 of the main text shows graphical representations of the results below.

Summary

PC	Eigenvalue	% Variance
1	2.7505	45.84%
2	1.6650	27.75%
3	1.1449	19.08%
4	0.2918	4.86%
5	0.1388	2.31%
6	0.0091	0.15%

Loadings

	PC 1	PC 2	PC 3	PC 4	PC 5	PC 6
$\delta^{18}O$	–0.539	0.143	0.309	0.230	0.526	0.513
$\delta^{13}C$	0.478	0.030	0.549	0.031	–0.397	0.557
Species	0.554	0.131	0.081	–0.416	0.703	–0.038
Origination	0.369	–0.462	–0.336	0.670	0.240	0.174
Extinction	0.178	0.685	0.185	0.560	0.021	–0.388
Global Sea Level	0.074	0.528	–0.670	–0.100	–0.112	0.494

Scores

	PC 1	PC 2	PC 3	PC 4	PC 5	PC 6
Danian	–1.1033	–1.0210	1.8230	0.1102	–0.2200	0.0468
Late Maastrichtian	–1.7642	–0.5295	0.6419	0.0490	0.3057	–0.0136
Early Maastrichtian	–1.4986	0.0203	–0.8796	–0.3091	–0.0516	–0.1841
Late Campanian	–1.2991	0.3897	–1.3673	–0.4192	–0.2684	0.1556
Middle Campanian	–0.0272	2.3654	0.0373	0.8106	0.2178	0.0119
Early Campanian	2.2494	1.1835	0.8917	–0.6160	–0.3501	–0.0358
Santonian	1.7537	–0.8274	–0.2722	–0.3828	0.6921	0.0371
Coniacian	1.6892	–1.5810	–0.8749	0.7572	–0.3255	–0.0180

Table S12. Results of principal component analysis for comparing possible controls on lamniform diversity dynamics using per-capita extinction and origination rates. Figure S3 of the Appendix shows a graphical representation of the results below.

Summary

PC	Eigenvalue	% Variance
1	3.0328	50.55%
2	1.8782	31.30%
3	0.6923	11.54%
4	0.3202	5.34%
5	0.0703	1.17%
6	0.0063	0.11%

Loadings

	PC 1	PC 2	PC 3	PC 4	PC 5	PC 6
$\delta^{18}O$	–0.520	–0.043	0.025	0.738	–0.142	0.403
$\delta^{13}C$	0.316	0.491	0.589	–0.014	0.203	0.521
Species	0.529	0.083	0.206	0.554	–0.378	–0.470
Origination	0.361	0.326	–0.735	0.268	0.347	0.177
Extinction	–0.417	0.480	0.153	0.130	0.492	–0.560
Global Sea Level	0.216	–0.643	0.215	0.244	0.658	–0.018

Scores

	PC 1	PC 2	PC 3	PC 4	PC 5	PC 6
Danian	–1.183	1.6277	0.0696	–0.1327	0.4701	1.3533
Late Maastrichtian	–1.238	0.3346	–0.1074	0.3877	–0.9318	–1.7417
Early Maastrichtian	–0.437	–1.1119	–0.5398	–0.4173	–1.2938	0.6974
Late Campanian	–0.265	–1.4275	–0.2823	–0.3328	0.6494	0.6528
Middle Campanian	–0.105	–0.6440	0.9581	1.3907	1.3177	–0.3677
Early Campanian	1.1961	0.3156	1.7799	–0.2290	–1.0371	0.2811
Santonian	1.4058	0.5943	–1.5566	1.1396	–0.1627	0.1215
Coniacian	0.6252	0.3113	–0.3215	–1.8061	0.9882	–0.9968

Table S13. Results of principal component analysis for comparing possible paleoenvironmental controls on hybodontiform diversity dynamics, using per-capita extinction and origination metrics. Figure S4 of the appendix shows a graphical representation of the results below.

Summary

PC	Eigenvalue	% Variance
1	3.2362	53.94%
2	1.9165	31.94%
3	0.4610	7.68%
4	0.2952	4.92%
5	0.0844	1.41%
6	0.0068	0.11%

Loadings

	PC 1	PC 2	PC 3	PC 4	PC 5	PC 6
$\delta^{18}O$	–0.475	–0.146	0.448	0.678	–0.127	0.277
$\delta^{13}C$	0.437	0.361	0.390	0.283	0.663	–0.082
Species	0.477	0.288	–0.124	0.464	–0.628	–0.253
Origination	–0.173	0.653	–0.419	0.061	0.053	0.601
Extinction	0.506	–0.214	0.357	–0.247	–0.238	0.673
Global Sea Level	0.264	–0.541	–0.574	0.424	0.300	0.196

Scores

	PC 1	PC 2	PC 3	PC 4	PC 5	PC 6
Danian	–1.4881	1.5439	0.2002	0.2155	0.8077	0.7336
Late Maastrichtian	–0.7551	–0.3723	1.7020	–0.2086	–0.9798	–0.6346
Early Maastrichtian	–0.5070	–0.9406	–0.3047	–0.6759	–0.8529	0.0560
Late Campanian	–0.3154	–1.2131	–1.0402	–0.1861	0.3240	1.3248
Middle Campanian	0.0947	–0.7402	–0.1533	1.8161	0.1960	–1.1570
Early Campanian	1.7677	0.1854	1.1425	0.2002	0.1950	1.1911
Santonian	0.5716	1.1914	–1.1998	0.5161	–1.5519	–0.3113
Coniacian	0.6314	0.3455	–0.3465	–1.6674	1.0789	–1.2027

Table S14. Table of mean values and 95% confidence intervals (CIs) for parameters shown in Fig. 10 of the main text.

	Lamniform Originations	Hybodontiform Originations	Lamniform Extinctions	Hybodontiform Extinctions	Global Sea levels	$\delta^{18}O$ (‰)	$\delta^{13}C_{carb}$ (‰)
Danian	—	—	—	—	194.80	-0.808	2.543
L. Maastrichtian	0.00	0.00	0.67	0.00	205.41	-0.543	2.284
E. Maastrichtian	0.00	0.00	0.14	0.00	218.68	-1.351	2.142
L. Campanian	0.00	0.00	0.13	0.00	226.11	-1.505	2.166
M. Campanian	0.00	0.00	0.43	1.00	225.58	-1.056	2.427
E. Campanian	0.06	0.00	0.18	0.60	217.09	-2.669	2.796
Santonian	0.47	0.60	0.06	0.00	212.84	-2.436	2.508
Coniacian	—	—	—	—	212.58	-2.943	2.513

95 % Confidence Intervals	Lamniform Originations		Hybodontiform Originations		Lamniform Extinctions		Hybodontiform Extinctions		Global Sea levels		$\delta^{18}O$ (‰)		$\delta^{13}C_{carb}$ (‰)	
	Lower	Upper	Lower	Upper	Lower	Upper	Lower	Upper	Lower	Upper	Lower	Upper	Lower	Upper
Danian	—	—	—	—	—	—	—	—	168.6	223.3	-0.9	-0.7	2.5	2.6
L. Maastrichtian	0.00	3.69	0.00	3.69	0.03	3.69	0.00	3.69	178.8	235.1	-0.7	-0.4	2.1	2.5
E. Maastrichtian	0.00	3.69	0.00	3.69	0.03	3.69	0.00	3.69	191.0	248.9	-1.5	-1.2	2.0	2.3
L. Campanian	0.00	3.69	0.00	3.69	0.03	3.69	0.00	3.69	198.4	257.5	-1.9	-1.1	2.0	2.4
M. Campanian	0.00	3.69	0.00	3.69	0.03	3.69	0.03	5.57	197.5	256.4	-1.4	-0.7	2.2	2.6
E. Campanian	0.03	3.69	0.00	3.69	0.03	3.69	0.03	3.69	190.0	247.9	-2.9	-2.5	2.6	3.0
Santonian	0.03	3.69	0.03	3.69	0.03	3.69	0.00	3.69	185.4	242.5	-2.9	-2.0	2.3	2.7
Coniacian	—	—	—	—	—	—	—	—	185.4	242.5	-3.6	-2.3	2.3	2.8

Fig. S1. Results of PCA (Fig. 13 of the main text) for comparing possible paleoenvironmental control of lamniform diversity dynamics using proportional extinction and origination datasets. **Top**: Loadings plot for correlation values of PC 1. **Bottom**: Scree plot for the percentage of eigenvalues, which indicates the first three components have large values (> 5.00%).

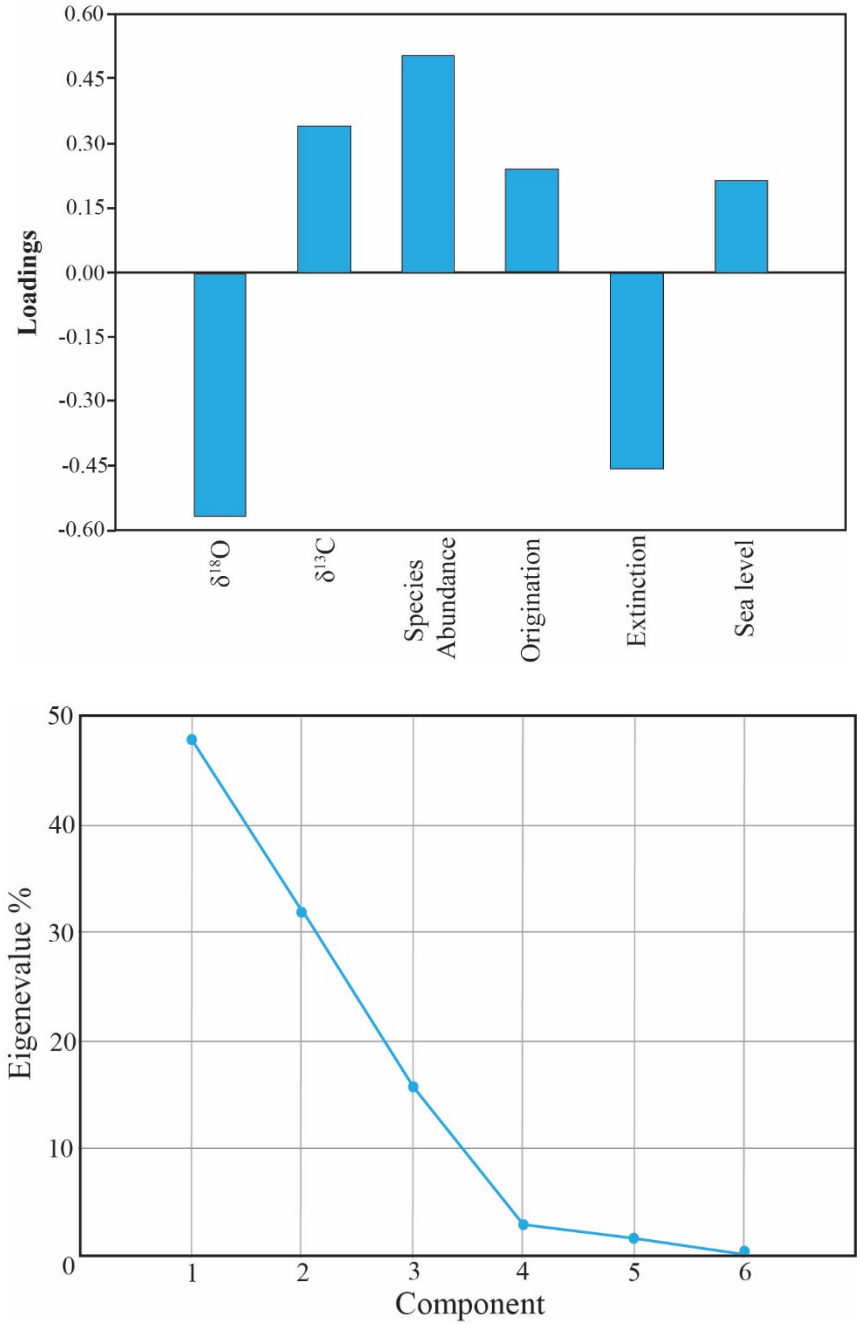

Fig. S2. Results of PCA (Fig. 14 of the main text) for comparing possible paleoenvironmental control of hybodontiform diversity dynamics using proportional extinction and origination datasets. **Top**: Loadings plot for correlation values of PC 1. **Bottom**: Scree plot for the percentage of eigenvalues, which indicates the first three components have large values (> 5.00%).

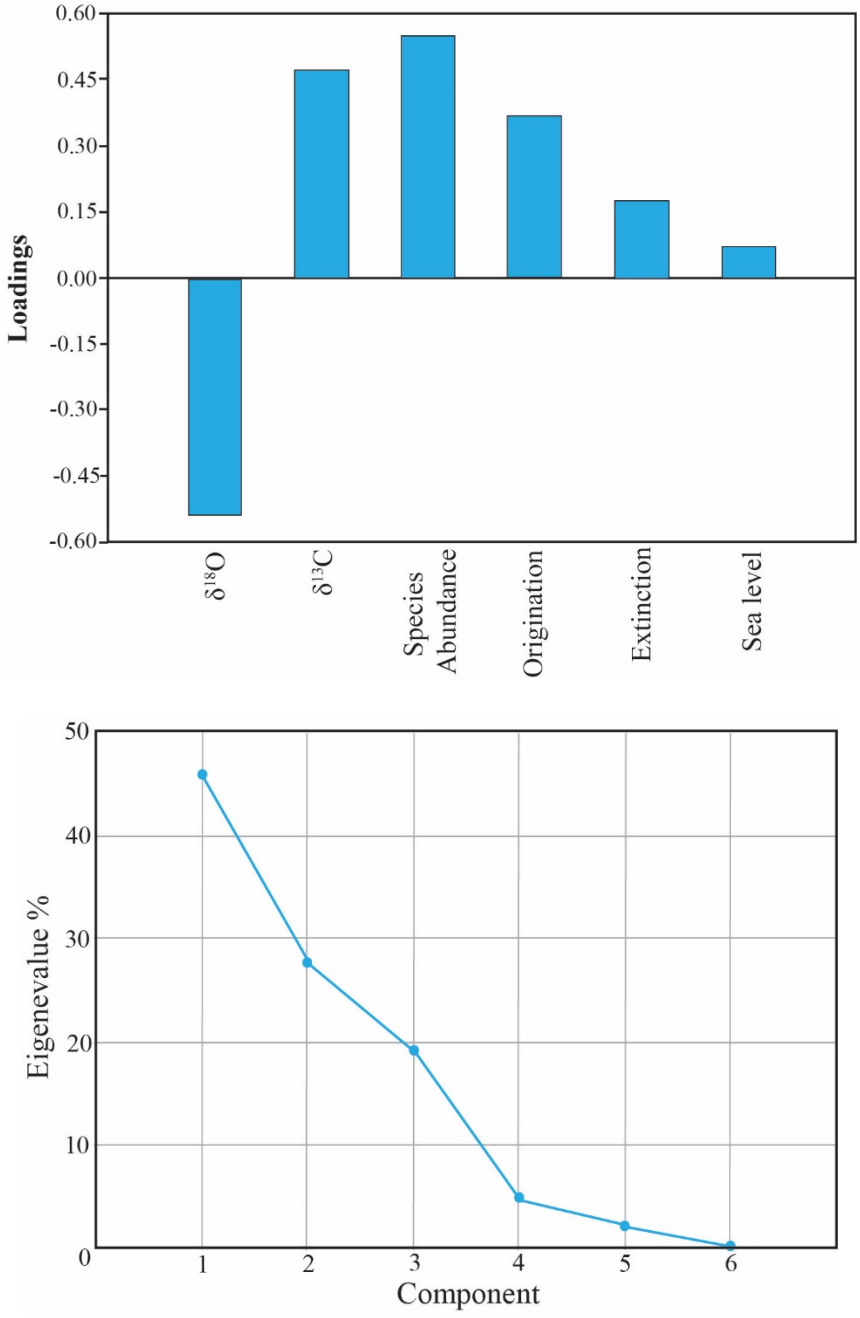

Fig. S3. PCA plot for possible controlling paleoenvironmental parameters of lamniform diversity dynamics, using per-capita extinction and origination rates, with respect to each of the eight time-bins.

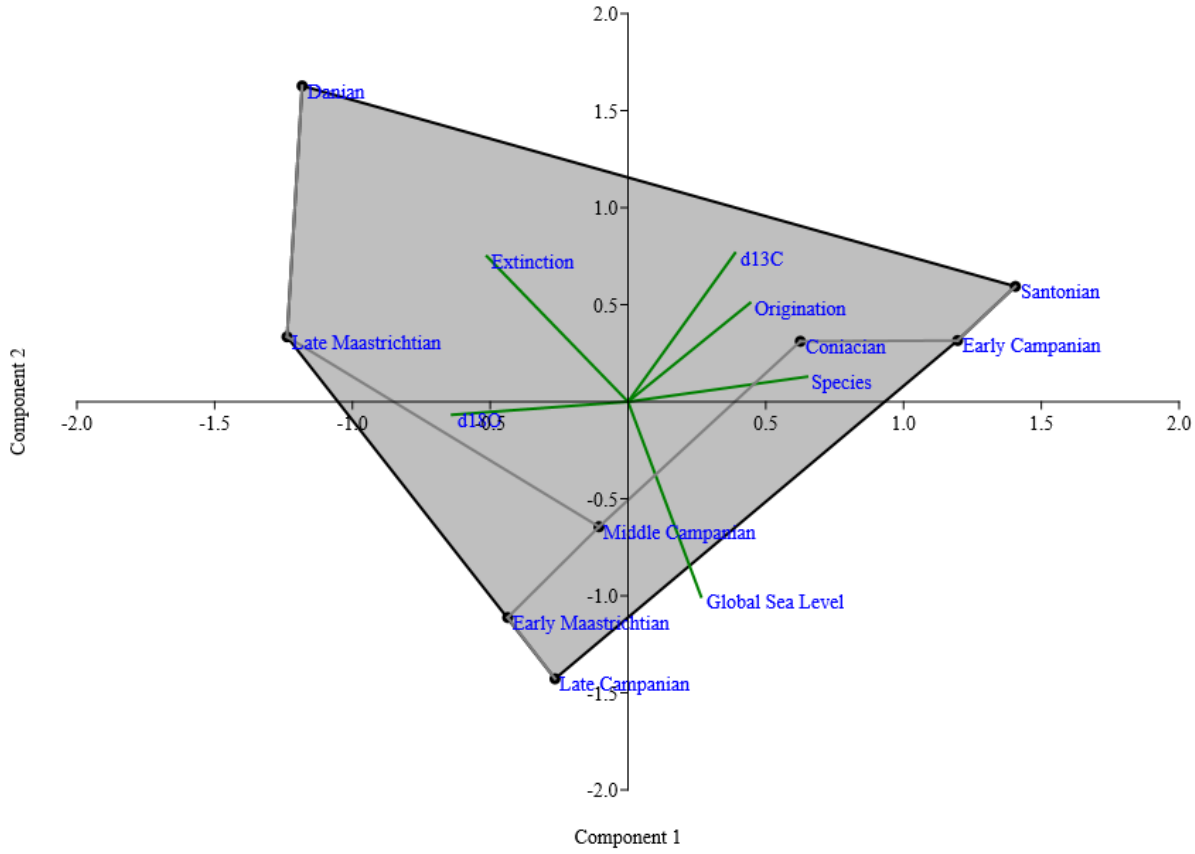

Fig. S4. Results of PCA for comparing possible paleoenvironmental controlling factors on lamniform diversity dynamics, using per-capita extinction and origination metrics. **Top**: Loadings plot for the correlation values of PC 1. **Bottom**: Scree plot of the percentages of eigenvalues, which indicates the first three components have large values (> 5.00%).

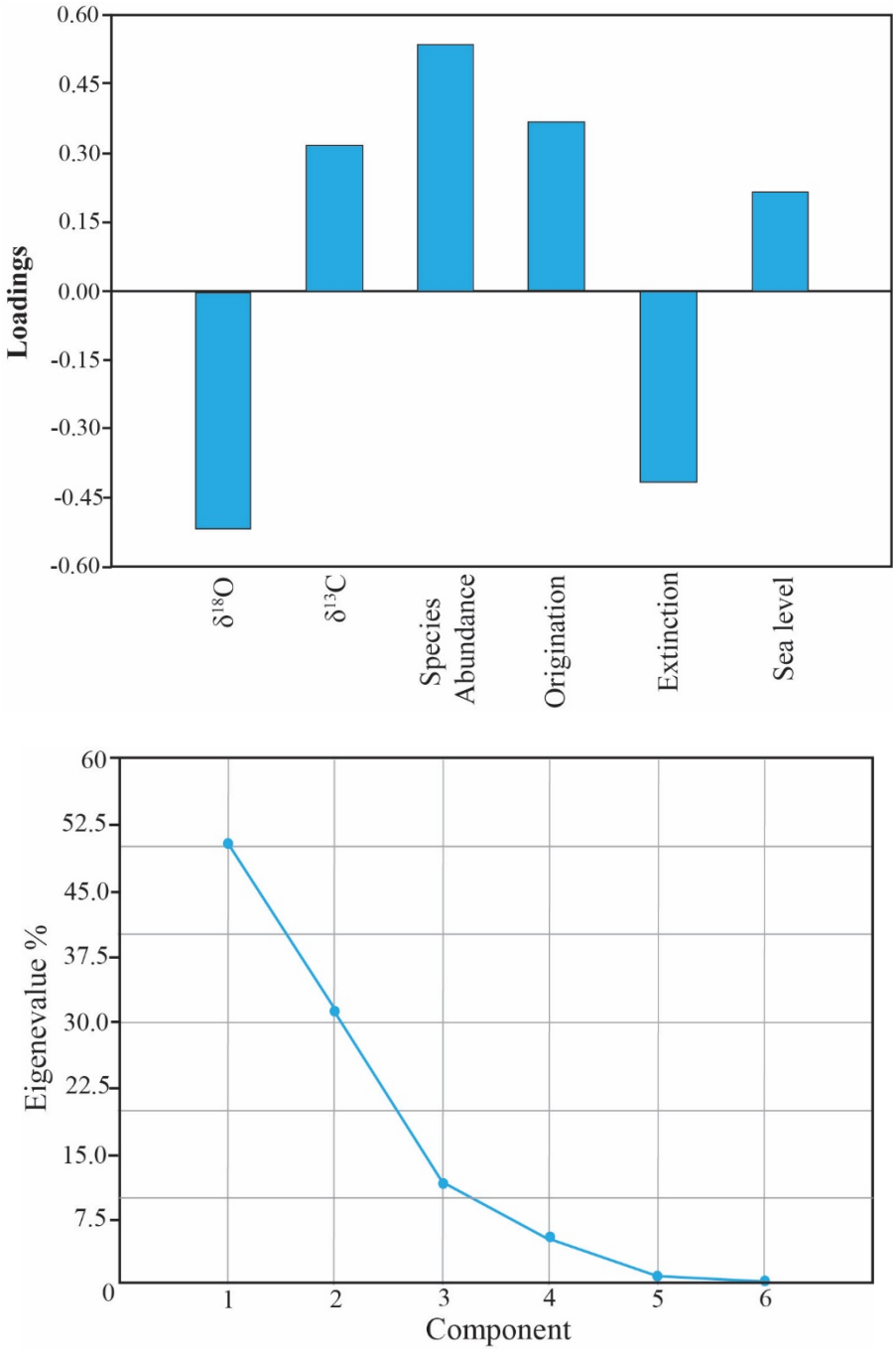

Fig. S5. PCA plot for possible controlling paleoenvironmental parameters on hybodontiform diversity dynamics, using per-capita extinction and origination metrics, with respect to each of the eight time-bins.

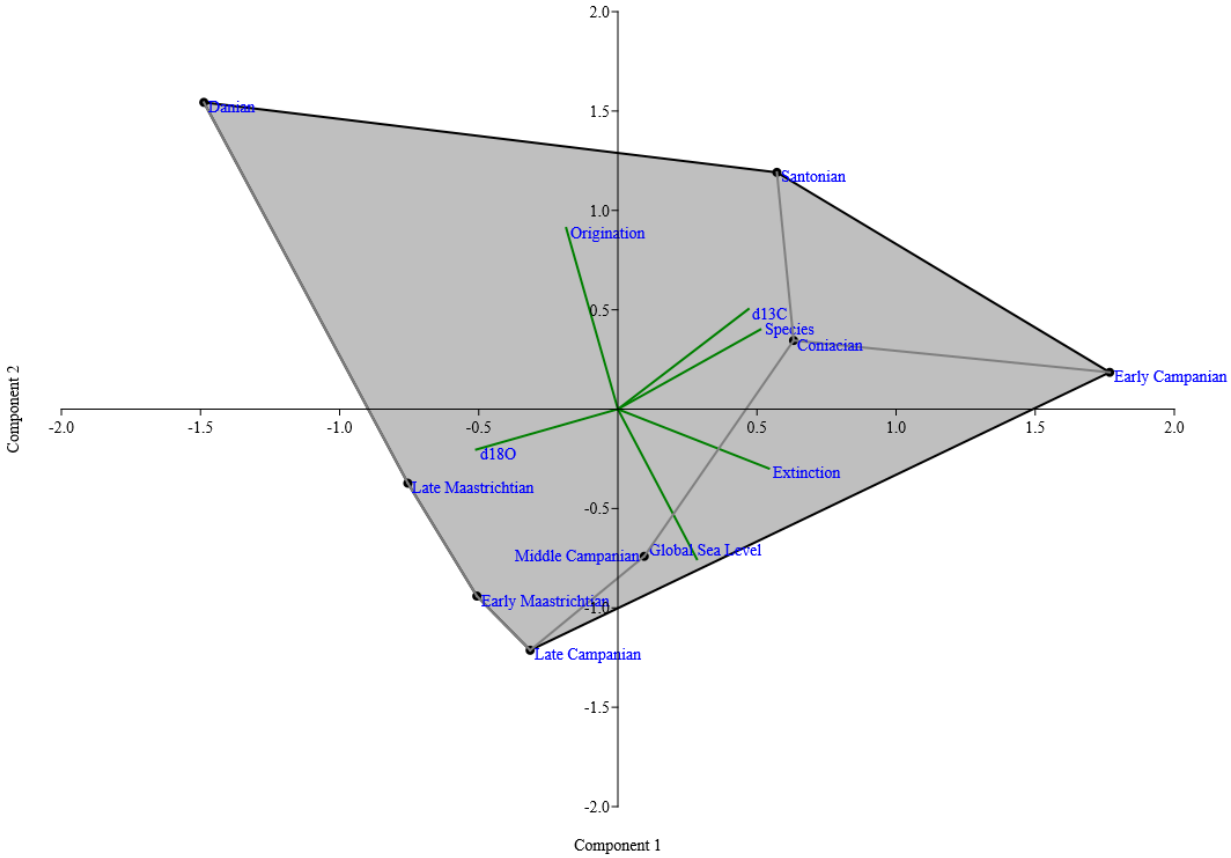

Fig. S6. Results of PCA for comparing possible paleoenvironmental controlling factors of hybodontiform diversity dynamics, using per-capita extinction and origination metrics. **Top**: Loadings plot for correlation values of PC 1. **Bottom**: Scree plot for the percentage of eigenvalues, which indicates the first three components have large values (< 5.00%).